Published in final edited form as:

*Traffic*. 2017 July ; 18(7): 465–484. doi:10.1111/tra.12485.

# Enzyme reversal to explore the function of yeast E3 ubiquitin-ligases

**Chris MacDonald**[1], **Stanley Winistorfer**[1], **R. Marshall Pope**[2], **Michael E. Wright**[1], and **Robert C. Piper**[1,*]

[1]Molecular Physiology and Biophysics, University of Iowa, Iowa City, IA USA 52242

[2]Proteomics Facility, University of Iowa, Iowa City, IA USA 52242

## Abstract

The covalent attachment of ubiquitin onto proteins can elicit a variety of downstream consequences. Attachment is mediated by a large array of E3 ubiquitin ligases, each thought be subject to regulatory control and to have a specific repertoire of substrates. Assessing the biological roles of ligases, and in particular, identifying their biologically relevant substrates has been a persistent yet challenging question. In this study we describe tools that may help achieve both of these goals. We describe a strategy whereby the activity of a ubiquitin ligase has been enzymatically reversed, accomplished by fusing it to a catalytic domain of an exogenous deubiquitinating enzyme. We present a library of 72 'anti-ligases' that appear to work in a dominant-negative fashion to stabilize their cognate substrates against ubiquitin-dependent proteasomal and lysosomal degradation. We then used the ligase-DUb library to screen for E3 ligases involved in post-Golgi / endosomal trafficking. We identify ligases previously implicated in these pathways (Rsp5 and Tul1), in addition to ligases previously localized to endosomes (Pib1 and Vps8). We also document an optimized workflow for isolating and analyzing the 'ubiquitome' of yeast, which can be used with mass-spectrometry to identify substrates perturbed by expression of particular ligase-DUb fusions.

### Keywords

Ubiquitin; E3 ubiquitin ligase; ubiquitination; lysosome; proteasome; ER-associated degradation (ERAD); endosomal trafficking; vacuolar protein sorting; mass spectrometry

## Introduction

Ubiquitination is a post-translational modification that controls almost every aspect of eukaryotic cell biology, including protein degradation, membrane trafficking, signal transduction, cell division, and DNA repair.[1-3] The conjugation of Ubiquitin (Ub) to either soluble proteins or the cytosolic portions of membrane proteins serves as a signal for protein degradation, carried out by either the proteasome or lysosome.[4,5] These activities maintain proper cellular levels of proteins and also provide a quality control mechanism to clear

*Correspondence: Robert-Piper@uiowa.edu.

misfolded proteins.[6] Different lysines within Ub itself can be ubiquitinated to create polyubiquitin chains of different topologies, which in turn can code for an enormous diversity in functional outcomes.[7] Typically, substrate lysine residues are conjugated to the C-terminal G76 residue of Ub upon transfer from E2 conjugating enzymes that carry Ub via a thiol-ester linkage. The vast majority of E3 ligases contain a RING (Really Interesting New Gene) domain and can bind E2 enzymes to direct their activity,[8] although other ligases such as HECT-type (Homologous to E6-AP Carboxyl Terminus) and RBR (Ring-Between-Ring) can themselves carry the thiol-ester linked Ub intermediate.

More than 600 predicted E3 enzymes are encoded in the human genome.[9] This diversity poses difficulties for studying ubiquitination; for example, ligase depletion/deletion experiments are often difficult to interpret due to redundancy of multiple ligases targeting the same substrate proteins. In addition, long-term ligase depletion/deletion studies may allow cells to adopt various compensatory responses or become enfeebled in the case of ligases that are essential for viability. These issues are compounded by technical problems, as it is inherently difficult to observe ubiquitinated protein species that are in the process of being degraded, and which account for only a small percentage of any protein population. Furthermore, ubiquitinated substrates are prone to deubiquitination during cell lysis procedures, when an array of deubiquitinating enzymes, which are notoriously difficult to inactivate, are unleashed [10]. *In vitro* approaches have greatly aided our understanding of the ubiquitination process, but generally fall short in preserving the level of specificity, diversity, and sensitivity needed to identify substrate candidates.

One of the best characterized E3 ligases in yeast is Rsp5, a HECT domain ligase of the NEDD4 (neural-precursor-cell-expressed, developmentally down-regulated) ligase family, which has multiple cellular roles.[11] Rsp5 has been intensely studied and proved a useful model for understanding human disease, such as alpha-Synuclein trafficking[12] and mechanisms driving catalysis of the NEDD4 ligases.[13,14] Although many putative ligases have no known substrates, Rsp5 has been implicated in the ubiquitination of ~80 substrates.[15-17] Rsp5 was originally identified as *npi1* (nitrogen permease inactivator 1) due to its role in downregulating cell surface transporters, such as Gap1 and Fur4.[18,19] Indeed, although Rsp5 has been shown to ubiquitinate proteasomal cargoes,[20] its broader function appears to be in modifying membrane proteins to provide a sorting signal for their delivery and degradation in the vacuole. Rsp5 is essential for viability owing to its role in controlling transcription of the enzyme required for oleic acid production.[21] Loss of function temperature-sensitive alleles have been useful tools to acutely inhibit Rsp5, however, different alleles appear to have varying levels of residual activity towards particular substrates.[22,23] Previously, we used an alternative approach to inhibit the function of Rsp5 that involved fusing the catalytic domain of a deubiquitinating enzyme (DUb) to the C-terminus of the ligase[24] and place production of this fusion protein under an inducible promoter. This dominant-negative Rsp5-DUb antagonizes endogenous Rsp5, illustrated by stabilization of a host of Rsp5 substrates.[24]

Here we apply this principle more widely by creating a systematic plasmid library of ligase-DUb fusion proteins. A survey of some of these ‘anti-ligases’ show that they antagonize the function of their endogenous counterpart, and do so with the sensitivity and specificity

required to perform future functional studies. In addition, we use this panel of anti-ligases to implicate new ubiquitin-dependent roles for Tul1, Pib1, and Vps8 in the sorting of the soluble hydrolase carboxypeptidase Y (CPY) to the vacuole. Finally, we present optimized methods and a yeast strain for proteomic analysis of the ubiquitinated portion of the yeast proteome, or “ubiquitome”. Our mass spectrometry analyses of purified ubiquitinated species indicates many components of the post-Golgi trafficking machinery, including many SNARE proteins, that may use ubiquitination to regulate their trafficking function. Furthermore, we quantitatively measure changes in ubiquitome levels following expression of the Pib1-DUb anti-ligase, to demonstrate the potential this combination of approaches has toward deciphering the function of Ub-ligases.

## Results & Discussion

### A systematic library of Ligase-DUb fusion proteins

A chimera of Rsp5 and the deubiquitinting enzyme (DUb) UL36 from the Herpes simplex virus I creates a dominant negative “anti-ligase” fusion protein that specifically deubiquitinates Rsp5 substrates.[24] We hypothesized this strategy could be applied to make an array of tools to probe the molecular functions of other E3 ligases (Figure 1A). We created a comprehensive E3 ligase-DUb plasmid library encoding ‘anti-ligases’, corresponding to each yeast open reading frame (ORF) predicted to encode an E3 ligase.[9] Each putative ligase was fused in frame to the UL36 catalytic domain and the HA epitope. The chimeras were housed in a *URA3*-containing plasmid and their expression placed under the inducible control of the *CUP1* promoter, allowing production in media supplemented with copper (Supplemental Figure S1a). Transforming the ligase-DUb expressing plasmids into yeast and immunoblotting extracts from two independent transformants with anti-HA confirmed expression and the correct predicted molecular weight for the set of ligase-DUb plasmids (Figure 1B). We found a few instances in which $Ura^+$ transformants did not express the HA-tagged ligase-DUb, emphasizing the importance of confirming expression of the ligase-DUb in future experiments. For a small subset of ligases, we could not recover plasmids that expressed detectable levels of a modified DUb-HA fusion counterpart (Supplemental Figure S1b & S1c).

To test whether particular DUb fusions elicit specific effects, we tested the ability of the ligase-DUbs to perturb cellular growth on their own or in combination with environmental stresses (Figure 2). Yeast transformants carrying each of the ligase-DUb plasmids grew comparably well in media containing low levels of copper (SD-Cu), where expression from the *CUP1* promoter was limited, or in media containing a copper chelator (SD+BCSA) to decrease *CUP1*-dependent expression even further. One exception was a modest reduction of growth in SD-Cu of cells expressing Hex3-DUb. This growth phenotype was not observed in SD-BCSA, but was dramatically exacerbated in media containing high 50 μM $CuCl_2$ to activate full production from the *CUP1* promoter (Figure 2A). Copper-induced expression of Rsp5-DUb resulted in a severe growth defect, whereas expression of Rtc1-DUb and Snt2-DUb caused obvious yet more modest growth defects. Similarly, cells expressing some ligase-DUbs had defects when exposed to increased temperature (37°C), alternate carbon sources, (oleate and/or ethanol/glycerol) or both (ethanol glycerol at 37°C). We also found

that mitochondrial morphology was aberrant in cells expressing DUb fusions of the F-box proteins Mfb1 and Mdm30, which have been previously implicated in regulating mitochondrial dynamics, with their loss causing mitochondria to fragment and aggregate.[25] Both Mfb1-DUb or Mdm30-DUb altered the ribbon morphology observed in wild-type cells to one that was fragmented (Figure 2B).

To directly demonstrate that a particular substrate could be targeted by its cognate ligase-DUb, we focused on two Rsp5 substrates, Sna3 and Cos5, that receive a ubiquitination signal that directs their sorting into the vacuolar lumen.[23,26,27] Both Sna3 and Cos5 bind Rsp5 directly (Figure 3A) and their mono- and di-ubiquitinated species can be detected as slower migrating species by SDS-PAGE and immunoblotting. As previously documented, expression of Rsp5-DUb disrupts the sorting of both Sna3 and Cos5,[23,27] demonstrated by GFP tagged versions localizing to endosomal structures instead of the vacuole lumen (Figure 3B). As expected, blocking the vacuolar degradation of Sna3 and Cos5 results in a large increase in steady state protein levels (Figure 3C). To compare the levels of ubiquitinated Sna3 and Cos5, we performed analysis in *vps36*Δ cells that are incapable of sorting these substrates into the vacuole for degradation. Because vacuolar degradation was blocked, levels of Sna3-HA and Cos5-HA in *vps36Δ* cells following expression of Rsp5-DUb were far more similar and allowed a clear comparison of the ubiquitinated species (Figure 3D). From this experiment, we found that the levels of ubiquitinated Sna3 and Cos5 were markedly depleted upon expression of the Rsp5-DUb anti-ligase (Figure 3E).

Collectively, these experiments show that each ligase-DUb fusion can be inducibly expressed by the addition of copper to the media and that they can elicit specific and potent phenotypes.

## Ligase-DUbs block degradation of substrates

We next tested whether other ligase-DUb fusions could specifically stabilize substrates, as we found for Rsp5-DUb (Figure 3,[24]). The ligase Hrd1 has a well-established role in ubiquitinating substrates for the ER-associated degradation (ERAD) pathway.[28,29] A model misfolded ERAD substrate is CPY*, a mutant form of CPY expressed by the *prc1-1* allele.[30] CPY* is ubiquitinated by Hrd1 at the ER and degraded by the proteasome.[6] We found inducing the expression of Hrd1-DUb caused a dramatic accumulation of CPY* (Figure 4A). This effect was specific to CPY* since no accumulation was observed for Pgk1 or the ER resident Dpm1. In addition, expressing various other DUb fusions had no significant impact on the levels of CPY*. We did note that addition of copper alone appears to decrease the levels of CPY*, although we did not pursue an explanation for this effect. Despite this effect of copper alone, it was clear that CPY* was greatly stabilized by Hrd1-DUb expression but not other ligase-DUbs (Supplemental Figure S2a). Expression of Hrd1-DUb also specifically blocked degradation of CPY* following a cycloheximide chase period (Figure 4B), a commonly used method to assess ERAD substrate degradation.[31]

The Grr1 ligase is known to target the cell cycle regulators Cln1 and Cln2, which are rapidly degraded by the proteasome.[32] Grr1 is one of many F-box proteins, which are the substrate binding subunit of a larger Skp1-Cullin-F-box architecture that forms an active Ub-ligase complex. We found that the levels of Cln1 and Cln2 are increased in both haploid and

diploid cells expressing Grr1-DUb, whereas expression of other ligase-DUbs had little effect (Figure 4C and Supplemental Figure S2b and S2c). In contrast, DUb fusion to another F-box protein, Cdc4, which targets Sic1 for degradation,[33,34] increased the levels of Sic1 but not Cln1.

## Ligases involved in post-Golgi membrane trafficking

We next used the library to screen for ligases that might be involved in endosomal membrane trafficking. We used two assays: first was a growth assay in media containing low tryptophan (Trp), which reveals a growth benefit to cells that can stabilize the high affinity tryptophan permease Tat2 at the cell surface. The second assay was secretion of the soluble vacuolar protease CPY, which serves as a general measure of proper sorting for many steps within the post-Golgi / endosomal pathway.[35]

For the Tat2 activity assay, we have previously documented that accelerated MVB sorting of Tat2 results in a growth defect in low Trp,[27] and reasoned that any ligases that exert influence on the ubiquitination status of Tat2 would result in a growth advantage (Figure 5A). Limiting Tryptophan resulted in a growth defect in cells expressing some ligase-DUb fusions but not others, emphasizing that different ligase-DUbs produce specific effects, further supporting data in Figure 2. The three ligase-DUbs that conferred the strongest growth advantage were those built with Pib1, Tul1 and Rsp5. Replicates of these DUb fusions show obvious growth enhancement when compared to vector alone (Figure 5B and C). The Rsp5-DUb fusion grows very poorly compared with vector control on minimal media containing copper, but this difference was almost entirely lost when cells are grown on low Trp media (Figure 5C), showing that despite the general growth defect in complete media, Rsp5-DUb allows cells to grow better in low Trp. The effect of Rsp5-DUb on growth in limited Trp is consistent with the known role of Rsp5 in targeting Tat2 for ubiquitination and Ub-dependent degradation in the vacuole.[36] The finding that Tul1-DUb gives enhanced growth in low Trp media also indicates reduced degradation of Tat2. This effect is consistent with previous studies implicating Tul1 in the ubiquitination and degradation of a variety of endosomal membrane proteins, such as mutant SNARE proteins and endogenous proteins, such as Phm5 and Cps1, which are well characterized cargoes that follow a Ub and ESCRT-dependent route to the vacuole.[37-39] The Pib1 ligase has previously localized to endosomal compartments via its PtdIns-3P binding FYVE (Fab1, YOTB, Vac1 and EEA1) domain,[40] consistent with the idea that Pib1-DUb perturbs Ub-dependent sorting of Tat2 through the MVB pathway to the vacuole. As confirmation that Tul1-DUb and Pib1-DUb have effects on ubiquitinated membrane protein cargoes, we found that their expression sensitized cells to canavanine, a toxic arginine analog that is transported through the Can1 permease (Figure 6A). Can1 is subject to ubiquitination and endocytosis to the vacuole; preventing ubiquitination stabilizes Can1 at the cell surface, which therefore allows for better canavanine transport and higher toxicity. Thus, these data are consistent with an effect of Tul1-DUb and Pib1-DUb to stabilize Can1 at the cell surface. We also found that mutating the active site cysteine with the DUb catalytic domain of Pib1 abolished this effect showing that canavanine-sensitivity requires active deubiquitination by Pib1-DUb. We also found that both Tul1-DUb and Pib1-DUb interrupted the normal delivery of Ste3-GFP along the MVB

pathway into the lumen of the vacuole (Figure 6B), again consistent with the idea that each of these ligase-DUbs can target endosomal membrane proteins.

We next evaluated the ligase-DUbs for effects on the sorting of CPY to the vacuole (Figure 7A and B). Despite extensive screening for proteins involved in this pathway,[35,41] an E3 ligase has not yet been implicated in the process. CPY secretion was measured using an immunoblot assay to detect secreted CPY from colonies over-layed with nitrocellulose filters. Mutant *vps4*Δ cells that secrete ~40% of their CPY,[35] were used as a comparative control. This assay revealed that expressing Pib1-DUb and Tul1-DUb caused mis-sorting of CPY. The CPY secretion defect upon expression of Pib1-DUb is unlikely due simply to the ability of Pib1 to associate with endosomes through its FYVE domain, as fusion of a DUb to ESCRT-0 (a complex of Hse1 and Vps27, the latter containing a FYVE domain) efficiently deubiquitinates Vps27, inhibits ESCRT recruitment and sorting of ubiquitinated MVB cargoes, but does not result in a CPY secretion defect.[24,42,43]

Our assay also showed that CPY was mis-sorted upon expression of DUb-fused Vps8, a CORVET specific subunit that plays an essential role in the vesicle biogenesis process, alongside Vps3 and the core Class C subunits, which are also the main components of the HOPS complex that drives homotypic fusion of the vacuolar membrane.[44] Yet DUb fusions with other HOPS/CORVET components that also have the RING domain signatures of Ub-ligases (Vps11 and Vps18) did not cause CPY secretion (Supplemental Figure S3). This suggests that Vps8 controls a Ub-dependent function when it is not in complex with other CORVET subunits.

In more general terms, our experiments uncover the existence of one or more Ub-dependent trafficking steps required for proper Tat2 trafficking and CPY sorting. Moreover, they implicate Pib1, Tul1, and Vps8 as ligases that contribute to this process. This is inferred from the dominant-negative effect that Pib1-DUb, Tul1-DUb, and Vps8-DUb have on endosomal sorting. The idea that this is due to perturbation of a ubiquitination event is supported by the observation that expressing Pib1, Tul1, or Vps8 fused to a catalytically dead deubiquitinase domain has no effect on CPY secretion (Figure 7C and D).

An important aspect of interpreting results from the ligase-DUb expression experiments is the model that these fusions work as dominant-negative alleles, perturbing the ubiquitination events catalyzed by endogenous ligases. Thus, even if a substrate is targeted by multiple ligases, only a single ligase-DUb is theoretically required to reverse those events. For Pib1 and Tul1, we confirmed earlier studies showing that single deletion of either *PIB1* or *TUL1* did not cause a Vps- (CPY secretion) phenotype (Figure 7E). To test whether redundancy amongst Pib1, Tul1, Vps8 and perhaps other Ub-ligases was responsible for the Ub-dependent effects of CPY sorting, we tested a series of combined mutants. A *pib1Δ tul1Δ* double mutant also did not secrete CPY, however, we could not recover double mutant cells that were capable of respiration on glycerol/ethanol plates, suggesting some type of genetic interaction (Supplemental Figure S4a). Since loss of Vps8 itself causes CPY secretion, combining *vps8*Δ with other mutations would not have been informative. We did make alleles in which the C-terminal RING finger was deleted or altered in hopes of retaining the bulk of Vps8 function whilst removing its Ub-specific function. However, these *vps8* alleles

did not complement CPY sorting (Supplemental Figure S4b). A CPY secretion phenotype for *pib1*Δ mutants was observed when the function of Rsp5 was also perturbed, by expressing Rsp5-DUb (Figure 7E). Although neither a *pib1*Δ mutant nor expression of Rsp5-DUb alone caused CPY secretion (Supplemental Figure S3), the combination did result in a low level of secretion, suggesting interplay between the endosomal ligases (Figure 7E).

Our observations using Pib1, Tul1, and Vps8 DUb fusions highlight an important caveat with interpreting results of using the ligase-DUb panel in general. On the one hand, the effect of a ligase-DUb could be that it directly antagonizes the effect of its endogenous wild-type ligase counterpart. This effect is consistent with what we observe for Hrd1-DUb, Grr1-DUb, Mfb1-DUb, and Rsp5-DUb and in line with the concept of a dominant-negative mutant. Alternatively, expression of a ligase-DUb could perturb the ubiquitination of a protein that is not a native substrate of the wild-type ligase. Even with this caveat, the ease of using the panel of ligase-DUbs to either follow the levels of a particular substrate (e.g. Cln2 or CPY*) or a biological function (e.g. Mitochondrial morphology or CPY sorting) make it an appealing way to identify candidate ligases that may play a role in a particular Ub-dependent process. Thus, these tools could provide new leads that can be followed up with more detailed analyses.

In the case of deciphering the role of Pib1, Tul1, or Vps8 in Ub-dependent steps that are required for proper sorting of vacuolar hydrolases, one way forward would be to determine how the repertoire of ubiquitinated proteins is altered by ligase-DUbs in order to find their candidate substrates, which in turn could shed light on the substrates of their endogenous wild-type ligase counterpart. Several protocols have been described for isolating and quantifying ubiquitinated proteins by mass-spectrometry. However, we found that these had problems in maximizing yield and purity of the ubiquitome. Therefore, we set out to optimize procedures for purifying pools of ubiquitinated proteins so that they could be easily compared to discover ligase-substrate relationships.

## A proteomic workflow for isolating and analyzing the ubiquitome

Optimizing the isolation of ubiquitinated proteins involved 3 main considerations: comprehensive cell lysis, a tight affinity tag for ubiquitinated proteins, and a simple yet very selective affinity purification scheme for enrichment. These pools of ubiqutinated proteins would then be subjected to tryptic digestion and LC-MS/MS. We felt a highly purified fraction was critical to the overall strategy since designating whether a protein is ubiquitinated, and then quantifying its abundance, could rely on measuring any peptide of that protein rather than only peptides containing remnants of lysine ubiquitination (a di-Glycine ‘stump’ that remains attached to the ubiquitinated lysine after trypsin digestion). This strategy would cast a wider net for identifying ubiquitinated proteins that might not contain enough detectable di-glycine peptides for quantitation, or that may have a plethora of ubiquitination sites that do not accurately reflect what proportion of a protein pool is ubiquitinated.

For extraction, the treatment of cells with alkali (0.2 N sodium hydroxide) prior to SDS lysis[45] was the most efficient extraction method that also significantly reduced the deubiquitination of modified species when cells or non-denatured lysates are incubated without energy renewal (Figures 8A and B). As originally described, NaOH / SDS prepared lysates are typically performed on small volumes of yeast. Because large quantities of lysates are required for downstream proteomic analysis, we confirmed that scaling up this procedure did not adversely affect reproducibility of extraction, as shown by immunoblotting the same amount amounts of lysates generated from 10 ml, 100 ml and 1000 ml cultures for marker proteins localized to the ER, cytosol and vacuole (Figure 8C). It was then crucial to remove SDS from samples so that they could be analyzed by LC-MS/MS. Previous methods describe a urea buffer exchange protocol using an ultrafiltration device.[46] Comparing this buffer exchange method with simple dialysis against urea buffer revealed dialysis removed SDS as quickly as centrifugal exchange, but with much less loss in overall protein levels (Figure 8D). This is an important consideration, as over 50% of sample was not recovered following buffer exchange. Considering, proteins of a certain size and / or hydrophobicity may be disproportionately lost during the removal of SDS, the landscape of the proteome could be significantly altered by not using dialysis, and it is therefore preferable to dialyze against large volumes of denaturing buffer. Even if proteins are depleted equally, this loss presents an unwieldy technical workflow to compensate.

We next focused on expression of 6xHistidine (His)-tagged Ub for capturing the ubiquitome. Procedures for isolating ubiquitinated proteins rely on expressing a 6xHis-tagged Ub in cells followed by affinity isolation of the 6xHis tag on Ni-NTA attached to sepharose.[47] Ni-NTA purification of 6xHis-ubiqutuinated proteins is advantageous because it can be done under denaturing conditions, specifically 8 M urea, which is the buffer into which our protein lysates are dialyzed. During our initial optimization of different commercially available Ub and His-tag antibodies it became apparent that anti-HisTag antibodies could not recognize 6xHis-Ub efficiently. Inserting a linker region of at least 6 or 8 amino acids was necessary to expose the epitope for immunodetection. Importantly, including this spacer also led to a considerable increase in the yield of purified ubiquitome, presumably by making the tag more accessible to the immobilized Ni-NTA (Figure 8E).

Using a single affinity isolation step to purify proteins on Ni-NTA sepharose was insufficient for eliminating non-specific proteins. This problem is exemplified by purifications from His-Ub expressing cells being indistinguishable from control cells lacking His-Ub, when assessed by silver staining of eluates. However, western blotting showed cells expressing His-Ub to be greatly enriched in ubiquitome. We found that a 2-step purification almost entirely removed this non-specific background. Two-step purification of His-Ub was relatively simple, as the initial elution was performed at low pH, followed by neutralization, binding to a smaller bed volume, washing, and imidazole elution, resulting in a much higher level of purification (Figure 8F and G). Indeed, the only remaining contaminants were identified as endogenous proteins that contain motifs mimicking His-tags, such as Snf1 that has 13 contiguous histidine residues in its N-terminal region and Hbt1 that contains multiple histidines within its C-terminal region (Figure 9C; Table 1).

We then built a yeast strain that expressed 6xHis-tagged Ub with an inserted 8 amino acid linker (6xHis-ALINQERA-Ub). Expression was from an engineered form of the *TEF1* promoter that yields a moderate level of expression.[48] Rather than replace all endogenous Ub genes with expression of 6xHis-Ub from a variable copy 2μ plasmid, as has been done is some previous studies, we integrated our expression construct in cells with either all 4 of their Ub-encoding genes intact, or integrating our construct at the *UBI4* locus to replace one of the main Ub-producing genes. We found that the loss of *UBI4* increased the overall yield of ubiquitinated proteins 5 fold (Figure 9A). We also deleted the *PDR5* gene, which encodes a broad-specificity efflux pump. This mutation sensitizes cells to drugs such as cycloheximide and increases the efficacy of the proteasomal inhibitor MG-132, which could be used in downstream experiments to accumulate proteasomal substrates (Figure 9B).

Of the endogenous protein contaminants following 2-step purification (Figure 9C), initial mass-spectrometry analysis of the ubiquitome fraction from these cells revealed that a major component was the contaminant protein Hbt1. This presented a significant problem because its abundance was so high that it interfered with the detection of other proteins within the sample. Hbt1 is a ~114 kDa protein that contains a C-terminal region with many tandem Histidine residues. Its ability to bind directly to Ni-NTA explains how it was found originally in studies looking for binding partners for His-tagged Hub1.[49] It was also the only protein identified in all 4 experimental replicates in a recent mass spectrometry study isolating His-Ub conjugates.[50] We sought to eliminate this contaminant to allow for a broader identification of peptides by mass spectrometry. Although the function of Hbt1 is not clear, we found that deletion of *HBT1* in the *ubi4Δ pdr5Δ* cells caused a growth defect (data not shown). As an alternative, we truncated the endogenous *HBT1* ORF, removing the C-terminal portion containing the native poly-histidine tag (Table 1) while retaining the majority (residues 1 - 996) of the protein-coding region. This manipulation has no effect on growth. Importantly, this eliminated the ability of Hbt1 to bind to Ni-NTA and removed it as a confounding contaminant in our ubiquitome samples (Figure 9D). Combining these approaches led to our final optimized purification protocol for affinity purifying the ubiquitome (Figure 9E).

To optimize the identification of ubiquitinated proteins by mass spectrometry, we found that recursive analyses performed on a modified exclusion list increased both the total number of proteins identified and the coverage of identified proteins (Figure 9F). This was done by subjecting a single sample to multiple rounds of LC-MS/MS using an Agilent 6520 Q-TOF instrument, and placing all of the successfully identified peptides on an exclusion list used to direct MS analysis in each subsequent round, as previously described.[51] This workflow was then used to perform 6 independent ubiquitome purifications, three under normal conditions and 3 in the presence of MG-132 to inhibit proteasomal degradation (Figure 9G), an approach that has been previously validated by mass spectrometry.[52] We identified almost 3000 proteins from these analyses. The relative levels of many of these were altered upon inhibition of the proteasome. Although not specifically targeted, this analysis also identified specific lysine residues containing a di-Gly stub, indicating some specific ubiquitination sites, some of which are novel; showing that the method enhancements described here will be useful for more detailed studies later. This analysis also highlighted several proteins that function in the endocytic pathway and could be targets of the Vps8-DUb, Pib1-DUb and/or

Tul1-DUb proteins that cause endosomal sorting defects (Table 2). These include a large number of SNARE proteins (Table 3), including Snc1, Snc2, Syn8, Vam3, Vti1 and Ykt6, which all function in membrane fusion events throughout the post-Golgi / endocytic system. Other proteins known to function in vacuolar protein sorting were also identified including components of the ESCRT apparatus as well as many proteins that help coordinate SNARE-mediated fusion including Vps8, Vps11, Vps18, and Vps45. Interestingly, Vps10, the sorting receptor for CPY that cycles between Golgi and endosomal compartments was identified within the ubiquitome. Alteration of the function of any of these proteins by ubiquitination could account for the perturbations we observe in the endocytic pathway upon expression of Pib1-DUb, Tul1-DUb, or Vps8-DUb and comparing changes within the ubiquitome upon their expression using the workflow described here should help narrow this candidate list. Intriguingly, although Rsp5 does not seem to be directly involved in the bulk of the ubiquitination required for these membrane trafficking steps, there was an additive effect of Rsp5-DUb in a *pib1Δ* background, suggesting that the function between the endosomal ligases is partially overlapping (Figure 7E).

The above described assays validate a role Rsp5 in endosomal ligase activity but suggest that other ligases, in particular Vps8, Pib1 and Tul1, collaborate to ubiquitinate components of the post-Golgi trafficking machinery, and this is required for upstream trafficking events, which subsequently converge with an Rsp5-dependent / MVB pathway. These additional ligases are all known to localize to endosomes and some have been reported to be active ligases.[38,40,53] The fact that, for example, *pib1Δ* cells do not have obvious sorting defects,[40] is in itself suggestive of a redundant role with another ligase.

## Alternations of the ubiquitome induced by Pib1-DUb

As a final exercise, we tested whether the ubiquitome isolation procedure was reproducible enough to examine the effects of ligase-DUb expression on the ubiquitome, using the Pib1-DUb anti-ligase as an example (Figure 10A). In order to assess changes in the ubiquitome it was tantamount to demonstrate that isolation of the ubiquitome, and subsequent analysis by LC-MS/MS, could yield reproducible results. This would be key so that changes induced by ligase-DUb expression could be reliably detected. For this evaluation we prepared biological replicates from two independent experiments from either control cells transformed with an empty vector or cells expressing Pib1-DUb (Figure 10B). Samples from cells lacking His-Ub were also analyzed to confirm efficient and specific purification of the ubiquitome. Tryptic fragments from ubiquitinated proteins were isolated before differential di-methyl labeling of amino groups using “light” and a “heavy” labels, as previously described (Figure 10C,[54]). Samples from vector control cells and Pib1-DUb-expressing cells were mixed at a 1:1 ratio and analyzed by LC-MS/MS using a Thermo Orbitrap Fusion Lumos instrument, with triplicate injections for each sample. Unlike the MS procedures described in Figure 9, this analysis did not employ additional chromatography steps before LC-MS/MS so as to simplify analysis and comparison of the replicate samples. Peptides were identified, quantified and compared and are listed in supplementary table S5. Over all the samples, 587 proteins were identified, however, for quantitation, only proteins that were found in multiple injections across both replicates were used for analysis by MaxQuant.[55] Also we also found a subset of proteins that were only found in either the ubiquitomes from control cells or

Pib1-DUb expressing cells (Figure 10D). We found that the levels of individual proteins within the ubiquitomes from two independent experiments were quite reproducible, for both control and Pib1-DUb samples (Figure 10E). Interestingly, expression of Pib1-DUb caused a subset of proteins to be reproducibly reduced from the ubiquitome (Figure 10F). Perhaps the most relevant finding regarding the utility of the ubiquitome isolation procedure and its combination with ligase-DUb treatment is that the levels of a large majority of identified proteins within the ubiquitomes were unchanged, which supports the overall reproducibility of these techniques and speaks to the specificity of ligase-DUbs. Second, was that this comparative proteomic approach identified changes in the levels of particular proteins within the ubiquitome of Pib1-DUb-expressing cells. Proteins that were less abundant in the ubiquitome of Pib1-DUb expressing cells could be directly deubiquitinated by Pib1-DUb, and thus qualify as potential substrates of endogenous Pib1. Alternatively, Pib1-DUb could work indirectly to somehow lower the steady-state levels of those proteins so that less are available for ubiquitination and recovery in the ubiquitome fraction. Proteins that are depleted from the ubiquitome of Pib1-DUb expressing cells include two Rsp5-adaptor proteins, Ecm21/Art2 and Art10, supporting the idea that Pib1 and Rsp5 have functional overlap or that Pib1 collaborates with Rsp5 to mediate ubiquitination of substrates of the endocytic / MVB pathway. Also identified were various plasma membrane transporters, including Tat1, Sam3, Opt1, and Fui1.[56-59] The idea that Pib1-DUb targets these transporters is consistent with the effects of Pib1-DUb on stabilizing Tat2 and Can1 (Figures 5 and 6) and implies a biological role for endogenous Pib1 in targeting a wide variety of cell surface proteins for ubiquitination and degradation in the vacuole. Erg11 (which is required for ergosterol synthesis[60]), and Mdm34 (a subunit of the ERMES complex required for mitochondrial-to-ER contact sites[61]), are also depleted in the Pib1-Dub ubiquitome relative to control, suggesting that Pib1 may play a novel role in lipid homeostasis and interorganelle contact.

## Summary

Here we describe a new tool to study the function of E3 Ub-ligases: a library expressing ligase-DUb ‘anti-ligases’ that correspond to most of the known yeast Ub ligases, and which appear to largely function in a dominant negative manner. This tool complements a variety of other approaches to study ligase function that together make a more effective approach to deciphering the roles of individual ligases. We also provide some enhancements and alternatives for isolating ubiquitinated proteins from yeast cells for subsequent identification and quantitation by mass-spectrometry or other downstream analyses, thus allowing the coupled use of ligase-DUb perturbation of the ubiquitome to find relevant ligase targets. Importantly, the effects of the ligase-DUb fusion proteins are considerably specific to the pathway or process in which the native ligase participates. Furthermore, the ability of ligase-DUbs to stabilize the cognate substrates of their endogenous counterpart provides a simple and convenient tool to identify the ligase(s) that mediate degradation of a particular substrate protein of interest. The utility of these ligase-DUbs as a discovery tool is documented by our studies and assays in endosomal trafficking, where we find that a Ub-dependent process is required for proper sorting of vacuolar hydrolases, and where we identify specific ligases and a number of candidate substrates that may effect this Ub-dependent process. The ligase-

DUb library, alongside the optimized reagents and protocols to biochemically assess the yeast ubiquitome, is a powerful tool to investigate the molecular mechanisms of many ubiquitination events that drive various cellular processes.

## Materials and Methods

### Reagents

The plasmids, yeast strains and antibodies used in this study are listed in supplemental tables 1 - 3.

### Cell culture conditions

Standard rich (YPD) and synesthetic complete (SC) media lacking appropriate base or amino acids were used throughout. Expression of plasmids under the control of the *CUP1* promoter was induced by the addition of 50 μM copper chloride to the media.

### CPY secretion assay

Yeast cells expressing ligase-DUb fusions were grown to mid-log phase in minimal media. Equivalent volumes of cells were harvested, spotted on a minimal media plate containing copper and grown overnight. Yeast were then replica plated on minimal media plates containing 50 μM copper chloride, dried and overlaid with a nitrocellulose membrane and grown at 30°C for 20 hours. Excess yeast were washed from membrane before immunoblotting with monoclonal anti-CPY antibodies as described.[43]

### Limited tryptophan growth assay

SEY6210 tryptohphan auxotroph (Trp-) cells expressing vector control or DUb-fusion plasmids were grown to mid-log phase in SC-Ura media before equivalent volumes harvested, washed in water and serially diluted (9:1) on plates of replete (40 μg/ml) and restricted (5 μg/ml and 2.5 μg/ml) Trp levels. This initial screening suggested ~60 ligase DUb fusions exhibited either reduced growth or had no growth advantage. ~20 fusions were selected for further analysis, which was performed as described above with additional platings on very low Trp plates (2 μg/ml, 1.5 μg/ml, 1 μg/ml, 0.5 μg/ml).

### Labeling of mitochondria

Yeast cells expressing labeled DUb fusion plasmids were grown to mid-log phase in SC-Ura media supplemented with either 2% glucose or 3% ethanol and 3% glycerol as a carbon source. Mitochondira staining was achieved by addition of 100 nM MitoTracker™ Red CMXRos dye to the cultures, which were grown at 30°C for 1 hour prior to washing with fresh media and imaging by fluorescence microscopy.

### Fluorescence microscopy

Yeast cells were grown to mid-log phase prior to resupension in “kill” buffer containing 100 mM Tris.HCl (pH 8.0), 0.2% (w/v) $NaN_3$ and NaF, prior to fluorescence microscopy, performed as previously described.[27]

### Immunoblot

Yeast cells harvested at mid-log phase were subjected to alkali treatment (0.2 N NaOH) for 3 minutes followed by resuspension in 50 mM Tris.HCl (pH 6.8), 5% SDS, 10% glycerol, and 8 M urea, to prepare whole cell lysates for SDS-PAGE. Immunoblotting was performed as previously described[23] using antibodies listed in supplemental table S3.

### Ubiquitome purification

A 2 litres culture of PLY4272 cells expressing His-ALINQERA-Ub was grown (per sample) to mid-log phase, harvested, treated for 3 minutes with 0.2 N NaOH prior to lysates being generated in denaturing buffer containing 50 mM Tris.HCl pH 8.0, 10% (w/v) glycerol, 5 mM β-Me 2.5% SDS and 8 M urea. Lysates were then diluted 20-30 fold in binding buffer (denaturing buffer lacking SDS), incubated for 2 hours at room temperature with 3 ml (50% slurry) $Ni^{2+}$-NTA agarose and collected in a column. Beads were washed with 10 × with binding buffer containing 10 mM imidazole and bound proteins eluted using 10 mls binding buffer at pH 4.5. Lysates were then neutralized (pH = 8.0) by addition of NaOH and incubated with a 300 µl (50% slurry) $Ni^{2+}$-NTA agarose for a further 2 hours. Bound proteins were then eluted in 1500 µl binding buffer containing 350 mM imidazole, dialysed against buffer lacking imidazole and then prepared for mass spectrometry. Samples from each stage in the process were removed, resuspended in Laemmli sample buffer, resolved by SDS-PAGE, and then subjected to silver staining or immunoblotting for visualiztion.

### Mass spectrometry sample preparation

Isolated ubiquitinated proteins were reduced by addition of 10 mM DTT powder for 1 hour at 37°C and then alkylated in 55 mM iodoacetamide for 1 hour at room temperature in the dark. Samples were diluted to 0.75 M urea with 50 mM Tris-HCl pH 8.5 and proteins digested with 20-µg trypsin (Promega) overnight at 37°C. Each sample was then spiked with a tryptic- digest of bovine serum albumin (BSA) at a 1:75 molar ratio with protein sample before acidification and desalting on C18 spin-columns. Samples were then fractionated by strong-cation exchange (SCX) on polysulfoethyl A packed spin columns. Briefly, desalted samples were dissolved into SCX buffer A (5 mM $KHPO_4$, 25% acetonitrile (ACN) and loaded onto SCX spin-columns. Peptides were eluted from the columns using a 12-step “salt-bump” protocol with buffer containing an increasing concentration of KCl (10, 15, 20, 25, 30, 35, 40, 45, 50, 55, 60, 120 mM), the gradient was created by mixing buffer A with buffer B (5 mM KHPO4, 25% ACN, 350 mM KCl). Eluted fractions were desalted, dried, and re-dissolved in mass spectrometry loading buffer (1% acetic acid, 1% ACN) and then analyzed by liquid chromatography tandem mass spectrometry (LC-MS/MS).

### Recursive mass spectrometry analysis

Trypsinized samples were analyzed by nano-liquid chromatography-tandem mass spectrometry using an Agilent 6520 Accurate-Mass Quadropole Time-of-Flight mass spectrometer interfaced with an HPLC Chip Cube. The samples were loaded onto an Ultra High Capacity Chip (500 nL enrichment column, 75 µm × 150 mm analytical column). LC-MS/MS analysis was performed using a 90-minute gradient ranging from 8 % to 35% buffer B (100% acetonitrile, 0.8% acetic acid). Full MS (MS1) data were acquired with a mass

range of 400 – 1250 m/z and acquisition rate of 1 spectra/second. From these data, an ion preferred list was generated with Agilent MassHunter Qualitative Software with the settings of 400-1250 m/z, 2+,3+, 4+, and 5+ charge states, and spectra with 2 or more ions. The directed Mass Spectrometry (dMS) was performed with the following settings: a maximum of 10 ions per cycle, a narrow isolation width (~ 1.3 atomic mass units), precursor masses dynamically excluded for 30 seconds after 8 MS/MS in a 30-second time window, and use of the preferred ion list. Mass spectrometry capillary voltage and capillary temperature settings were set to 1800 V and 330°C, respectively. The infused reference mass of 1221.9906 was used to correct precursor m/z masses each LC-MS/MS experiment.

For protein identification, the raw.d files were searched against the UniProt mouse database using SpectrumMill Software version B.04.01.141 (Agilent Technologies) with the following settings: precursor mass tolerance of 25 parts per million (ppm), product mass tolerance of 200 ppm, maximum of 2 miss cleavages, maximum charge state +5, minimum parent mass shift -18 AMU and maximum parent mass shift 250 AMU. Search modifications included static carbamidomethylation on cysteine residues (C = 57.02 AMU) and variable modifications for oxidized methionine (M = 15.99 AMU), STY phosphorylation (STY = 79.966 AMU), and ubiquitination (GG = 114.043 AMU). The search results with a <1% false discovery rate were accepted and converted to a scaffold file for data interpretation.

### Dimethyl Labeling of peptides

Samples were reduced with DTT, alkylated with chloroacetamide and then diluted for digestion first with Lys C and then Trypsin. N-terminal amines and lysine residues were tagged using reductive amination with isotopic variants of formaldehyde, as previously described.[54] MALDI analysis of the total peptide content for each sample was then used to mix heavy and light samples at a 1:1 ratio.

### Comparative analysis of dimethyl-labeled peptides

The University of Iowa Proteomic Facility performed dimethyl labeling and analysis of peptides in Figure 10. Each labeled (‘light’ and ‘heavy’) peptide mixture was loaded on home-packed C-18 column (Halo 2.7 μm particles: MDC) 100 μm i.d. × 10 cm using the Thermo EZ nLC 1200 and analyzed on an Orbitrap Fusion Lumos mass spectrometer (Thermo Fisher Scientific, San Jose, CA). For each injection, an estimated 0.5 μg of total peptide was loaded and followed though a 120 minute linear gradient of 0% to 95% ACN in 0.1% Formic acid.

Full MS (MS1) data were acquired with a mass range of 350 -1500 m/z at a resolution of 60,000. The most abundant precursors were selected among 2-8 charge state ions at a 2.0E5 threshold, isolated by a multi-segment quadrupole with a mass window of m/z 2, and sequentially subjected to both CID and HCD fragmentation. Ions were then dynamically excluded for 30 seconds. Both MS2 channels were recorded as centroid and the MS1 survey scans were recorded in profile mode.

Initial spectral searches were performed with MaxQuant v. 1.5.1[55] against UniprotKB entries for the organism *Saccharomyces cerevisiae* NCBI taxonomy no. 559292 and with the

Byonic (Protein Metrics) ver. 2.8.2. In either search an equal number of decoy entries were created and searched simultaneously by reversing the original entries in the Target databases. Discriminant scores were determined by Scaffold Q+S ver. 4.7 (Proteome Software) at 2% FDR.

## Supplementary Material

Refer to Web version on PubMed Central for supplementary material.

## Acknowledgments

We would like to thank Markus Abei for the *prc1-1* strain, Christian Ungermann and Scott Moye-Rowley for helpful discussions, and William Smith for technical help with composing the ligase-DUb library. We would like to thank Jordy Hsiao and Harryl Martinez, in the laboratory of ME Wright, for help with recursive mass spectrometry analysis and operation of the Agilent 6520 Q-TOF. This work was supported by the NIH (5R01GM058202 and R01GM094830) and by an AHA postdoctoral fellowship award (15POST22980010) to CM. The comparative analysis with dimethyl-labeled samples was performed in the University of Iowa Proteomic facility, supported by an endowment from the Carver Foundation and by a Thermo Lumos provided by a grant to Dr. Kevin Campbell.

## References

1. Glickman MH, Ciechanover A. The ubiquitin-proteasome proteolytic pathway: destruction for the sake of construction. Physiological Reviews. 2002; 82(2):373–428. DOI: 10.1152/physrev.00027.2001 [PubMed: 11917093]
2. Mukhopadhyay D, Riezman H. Proteasome-Independent Functions of Ubiquitin in Endocytosis and Signaling. Science. 2007; 315(5809):201–205. DOI: 10.1126/science.1127085 [PubMed: 17218518]
3. Popovic D, Vucic D, Dikic I. Ubiquitination in disease pathogenesis and treatment. Nat Med. 2014; 20(11):1242–1253. DOI: 10.1038/nm.3739 [PubMed: 25375928]
4. Ravid T, Hochstrasser M. Diversity of degradation signals in the ubiquitin-proteasome system. Nat Rev Mol Cell Biol. 2008; 9(9):679–690. DOI: 10.1038/nrm2468 [PubMed: 18698327]
5. Piper RC, Dikic I, Lukacs GL. Ubiquitin-dependent sorting in endocytosis. Cold Spring Harbor Perspectives in Biology. 2014; 6(1):a016808.doi: 10.1101/cshperspect.a016808 [PubMed: 24384571]
6. Ruggiano A, Foresti O, Carvalho P. Quality control: ER-associated degradation: protein quality control and beyond. J Cell Biol. 2014; 204(6):869–879. DOI: 10.1083/jcb.201312042 [PubMed: 24637321]
7. Komander D, Rape M. The ubiquitin code. Annu Rev Biochem. 2012; 81:203–229. DOI: 10.1146/annurev-biochem-060310-170328 [PubMed: 22524316]
8. Deshaies RJ, Joazeiro CAP. RING domain E3 ubiquitin ligases. Annu Rev Biochem. 2009; 78:399–434. DOI: 10.1146/annurev.biochem.78.101807.093809 [PubMed: 19489725]
9. Li, W., Bengtson, MH., Ulbrich, A., et al. Genome-wide and functional annotation of human E3 ubiquitin ligases identifies MULAN, a mitochondrial E3 that regulates the organelle's dynamics and signaling. In: Ploegh, H., editor. PLoS ONE. Vol. 3. 2008. p. e1487
10. Katzmann, DJ., Wendland, B. Ubiquitin and Protein Degradation, Part B. Vol. 399. Elsevier; 2005. Analysis of Ubiquitin-Dependent Protein Sorting Within the Endocytic Pathway in Saccharomyces cerevisiae; p. 192-211.p. 99013-7.Methods in Enzymology
11. Huibregtse JM, Scheffner M, Beaudenon S, Howley PM. A family of proteins structurally and functionally related to the E6-AP ubiquitin-protein ligase. Proc Natl Acad Sci USA. 1995; 92(7):2563–2567. [PubMed: 7708685]
12. Tardiff DF, Jui NT, Khurana V, et al. Yeast reveal a “druggable” Rsp5/Nedd4 network that ameliorates α-synuclein toxicity in neurons. Science. 2013; 342(6161):979–983. DOI: 10.1126/science.1245321 [PubMed: 24158909]

13. Kamadurai HB, Souphron J, Scott DC, et al. Insights into Ubiquitin Transfer Cascades from a Structure of a UbcH5B~Ubiquitin-HECTNEDD4L Complex. Mol Cell. 2009; 36(6):1095–1102. DOI: 10.1016/j.molcel.2009.11.010 [PubMed: 20064473]
14. Kamadurai, HB., Qiu, Y., Deng, A., et al. Mechanism of ubiquitin ligation and lysine prioritization by a HECT E3. In: Kuriyan, J., editor. eLife. Vol. 2. 2013. p. e00828
15. Kus B, Gajadhar A, Stanger K, et al. A High Throughput Screen to Identify Substrates for the Ubiquitin Ligase Rsp5. J Biol Chem. 2005; 280(33):29470–29478. DOI: 10.1074/jbc.M502197200 [PubMed: 15955809]
16. Gupta R, Kus B, Fladd C, et al. Ubiquitination screen using protein microarrays for comprehensive identification of Rsp5 substrates in yeast. Mol Syst Biol. 2007; 3doi: 10.1038/msb4100159
17. Lee WC, Lee M, Jung JW, Kim KP, Kim D. SCUD: Saccharomyces cerevisiae ubiquitination database. BMC Genomics. 2008; 9:440.doi: 10.1186/1471-2164-9-440 [PubMed: 18811980]
18. Vandenbol M, Jauniaux JC, Vissers S, Grenson M. Isolation of the NPR1 gene responsible for the reactivation of ammonia-sensitive amino-acid permeases in Saccharomyces cerevisiae. RNA analysis and gene dosage effects. Eur J Biochem. 1987; 164(3):607–612. [PubMed: 3552673]
19. Hein C, Springael JY, Volland C, Haguenauer-Tsapis R, Andre B. NPl1, an essential yeast gene involved in induced degradation of Gap1 and Fur4 permeases, encodes the Rsp5 ubiquitin-protein ligase. Mol Microbiol. 1995; 18(1):77–87. [PubMed: 8596462]
20. Fang NN, Chan GT, Zhu M, et al. Rsp5/Nedd4 is the main ubiquitin ligase that targets cytosolic misfolded proteins following heat stress. Nat Cell Biol. 2014; 16(12):1227–1237. DOI: 10.1038/ncb3054 [PubMed: 25344756]
21. Chellappa R, Kandasamy P, Oh CS, Jiang Y, Vemula M, Martin CE. The membrane proteins, Spt23p and Mga2p, play distinct roles in the activation of Saccharomyces cerevisiae OLE1 gene expression. Fatty acid-mediated regulation of Mga2p activity is independent of its proteolytic processing into a soluble transcription activator. J Biol Chem. 2001; 276(47):43548–43556. DOI: 10.1074/jbc.M107845200 [PubMed: 11557770]
22. Kee Y, Muñoz W, Lyon N, Huibregtse JM. The deubiquitinating enzyme Ubp2 modulates Rsp5-dependent Lys63-linked polyubiquitin conjugates in Saccharomyces cerevisiae. J Biol Chem. 2006; 281(48):36724–36731. DOI: 10.1074/jbc.M608756200 [PubMed: 17028178]
23. MacDonald C, Stringer DK, Piper RC. Sna3 Is an Rsp5 Adaptor Protein that Relies on Ubiquitination for Its MVB Sorting. Traffic. 2012; 13(4):586–598. DOI: 10.1111/j.1600-0854.2011.01326.x [PubMed: 22212814]
24. Stringer DK, Piper RC. A single ubiquitin is sufficient for cargo protein entry into MVBs in the absence of ESCRT ubiquitination. J Cell Biol. 2011; 192(2):229–242. DOI: 10.1083/jcb.201008121 [PubMed: 21242292]
25. Dürr M, Escobar-Henriques M, Merz S, Geimer S, Langer T, Westermann B. Nonredundant roles of mitochondria-associated F-box proteins Mfb1 and Mdm30 in maintenance of mitochondrial morphology in yeast. Mol Biol Cell. 2006; 17(9):3745–3755. DOI: 10.1091/mbc.E06-01-0053 [PubMed: 16790496]
26. Oestreich AJ, Aboian M, Lee J, et al. Characterization of multiple multivesicular body sorting determinants within Sna3: a role for the ubiquitin ligase Rsp5. Mol Biol Cell. 2007; 18(2):707–720. DOI: 10.1091/mbc.E06-08-0680 [PubMed: 17182849]
27. MacDonald C, Payne JA, Aboian M, Smith W, Katzmann DJ, Piper RC. A family of tetraspans organizes cargo for sorting into multivesicular bodies. Developmental Cell. 2015; 33(3):328–342. DOI: 10.1016/j.devcel.2015.03.007 [PubMed: 25942624]
28. Gardner RG, Swarbrick GM, Bays NW, et al. Endoplasmic reticulum degradation requires lumen to cytosol signaling. Transmembrane control of Hrd1p by Hrd3p. J Cell Biol. 2000; 151(1):69–82. [PubMed: 11018054]
29. Bays NW, Gardner RG, Seelig LP, Joazeiro CA, Hampton RY. Hrd1p/Der3p is a membrane-anchored ubiquitin ligase required for ER-associated degradation. Nat Cell Biol. 2001; 3(1):24–29. DOI: 10.1038/35050524 [PubMed: 11146622]
30. Wolf DH, Fink GR. Proteinase C (carboxypeptidase Y) mutant of yeast. J Bacteriol. 1975; 123(3):1150–1156. [PubMed: 51020]

31. Gardner RG, Hampton RY. A “distributed degron” allows regulated entry into the ER degradation pathway. EMBO J. 1999; 18(21):5994–6004. DOI: 10.1093/emboj/18.21.5994 [PubMed: 10545111]
32. Li FN, Johnston M. Grr1 of Saccharomyces cerevisiae is connected to the ubiquitin proteolysis machinery through Skp1: coupling glucose sensing to gene expression and the cell cycle. EMBO J. 1997; 16(18):5629–5638. DOI: 10.1093/emboj/16.18.5629 [PubMed: 9312022]
33. Schwob E, Böhm T, Mendenhall MD, Nasmyth K. The B-type cyclin kinase inhibitor p40SIC1 controls the G1 to S transition in S. cerevisiae. Cell. 1994; 79(2):233–244. [PubMed: 7954792]
34. Verma R, Annan RS, Huddleston MJ, Carr SA, Reynard G, Deshaies RJ. Phosphorylation of Sic1p by G1 Cdk required for its degradation and entry into S phase. Science. 1997; 278(5337):455–460. [PubMed: 9334303]
35. Raymond CK, Howald-Stevenson I, Vater CA, Stevens TH. Morphological classification of the yeast vacuolar protein sorting mutants: evidence for a prevacuolar compartment in class E vps mutants. Mol Biol Cell. 1992; 3(12):1389–1402. [PubMed: 1493335]
36. Abe F, Iida H. Pressure-induced differential regulation of the two tryptophan permeases Tat1 and Tat2 by ubiquitin ligase Rsp5 and its binding proteins, Bul1 and Bul2. Mol Cell Biol. 2003; 23(21):7566–7584. [PubMed: 14560004]
37. Tong Z, Kim MS, Pandey A, Espenshade PJ. Identification of Candidate Substrates for the Golgi Tul1 E3 Ligase Using Quantitative diGly Proteomics in Yeast. Molecular & Cellular Proteomics. 2014; 13(11):2871–2882. DOI: 10.1074/mcp.M114.040774 [PubMed: 25078903]
38. Reggiori F, Pelham HRB. A transmembrane ubiquitin ligase required to sort membrane proteins into multivesicular bodies. Nat Cell Biol. 2002; 4(2):117–123. DOI: 10.1038/ncb743 [PubMed: 11788821]
39. Taubas JV, Pelham H. Swf1-dependent palmitoylation of the SNARE Tlg1 prevents its ubiquitination and degradation. EMBO J. 2005; 24(14):2524–2532. DOI: 10.1038/sj.emboj.7600724 [PubMed: 15973437]
40. Shin ME, Ogburn KD, Varban OA, Gilbert PM, Burd CG. FYVE domain targets Pib1p ubiquitin ligase to endosome and vacuolar membranes. J Biol Chem. 2001; 276(44):41388–41393. DOI: 10.1074/jbc.M105665200 [PubMed: 11526110]
41. Bonangelino CJ, Chavez EM, Bonifacino JS. Genomic screen for vacuolar protein sorting genes in Saccharomyces cerevisiae. Mol Biol Cell. 2002; 13(7):2486–2501. DOI: 10.1091/mbc.02-01-0005 [PubMed: 12134085]
42. Bilodeau PS, Urbanowski JL, Winistorfer SC, Piper RC. The Vps27p–Hse1p complex binds ubiquitin and mediates endosomal protein sorting. Nat Cell Biol. Jun.2002 doi: 10.1038/ncb815
43. MacDonald C, Buchkovich NJ, Stringer DK, Emr SD, Piper RC. Cargo ubiquitination is essential for multivesicular body intralumenal vesicle formation. EMBO Rep. 2012; 13(4):331–338. DOI: 10.1038/embor.2012.18 [PubMed: 22370727]
44. Balderhaar HJK, Ungermann C. CORVET and HOPS tethering complexes - coordinators of endosome and lysosome fusion. J Cell Sci. 2013; 126(Pt 6):1307–1316. DOI: 10.1242/jcs.107805 [PubMed: 23645161]
45. Kushnirov VV. Rapid and reliable protein extraction from yeast. Yeast. 2000; 16(9):857–860. DOI: 10.1002/1097-0061(20000630)16:9<857::AID-YEA561>3.0.CO;2-B [PubMed: 10861908]
46. Wiśniewski JR, Zougman A, Nagaraj N, Mann M. Universal sample preparation method for proteome analysis. Nat Methods. 2009; 6(5):359–362. DOI: 10.1038/nmeth.1322 [PubMed: 19377485]
47. Peng J, Schwartz D, Elias JE, et al. A proteomics approach to understanding protein ubiquitination. Nat Biotechnol. 2003; 21(8):921–926. DOI: 10.1038/nbt849 [PubMed: 12872131]
48. Nevoigt E, Kohnke J, Fischer CR, Alper H, Stahl U, Stephanopoulos G. Engineering of Promoter Replacement Cassettes for Fine-Tuning of Gene Expression in Saccharomyces cerevisiae. Applied and Environmental Microbiology. 2006; 72(8):5266–5273. DOI: 10.1128/AEM.00530-06 [PubMed: 16885275]
49. Dittmar GAG, Wilkinson CRM, Jedrzejewski PT, Finley D. Role of a ubiquitin-like modification in polarized morphogenesis. Science. 2002; 295(5564):2442–2446. DOI: 10.1126/science.1069989 [PubMed: 11923536]

50. Fang NN, Ng AHM, Measday V, Mayor T. Hul5 HECT ubiquitin ligase plays a major role in the ubiquitylation and turnover of cytosolic misfolded proteins. Nat Cell Biol. 2011; 13(11):1344–1352. DOI: 10.1038/ncb2343 [PubMed: 21983566]
51. Hsiao JJ, Smits MM, Ng BH, Lee J, Wright ME. Discovery Proteomics Identifies a Molecular Link between the Coatomer Protein Complex I and Androgen Receptor-dependent Transcription. J Biol Chem. Jun.2016 jbc.M116.732313. doi: 10.1074/jbc.M116.732313
52. Xu P, Duong DM, Seyfried NT, et al. Quantitative proteomics reveals the function of unconventional ubiquitin chains in proteasomal degradation. Cell. 2009; 137(1):133–145. DOI: 10.1016/j.cell.2009.01.041 [PubMed: 19345192]
53. Horazdovsky BF, Cowles CR, Mustol P, Holmes M, Emr SD. A novel RING finger protein, Vps8p, functionally interacts with the small GTPase, Vps21p, to facilitate soluble vacuolar protein localization. J Biol Chem. 1996; 271(52):33607–33615. [PubMed: 8969229]
54. Yu CL, Summers RM, Li Y, Mohanty SK, Subramanian M, Pope RM. Rapid identification and quantitative validation of a caffeine-degrading pathway in Pseudomonas sp. CES. J Proteome Res. 2015; 14(1):95–106. DOI: 10.1021/pr500751w [PubMed: 25350919]
55. Cox J, Mann M. MaxQuant enables high peptide identification rates, individualized p.p.b.-range mass accuracies and proteome-wide protein quantification. Nat Biotechnol. 2008; 26(12):1367–1372. DOI: 10.1038/nbt.1511 [PubMed: 19029910]
56. Schmidt A, Hall MN, Koller A. Two FK506 resistance-conferring genes in Saccharomyces cerevisiae, TAT1 and TAT2, encode amino acid permeases mediating tyrosine and tryptophan uptake. Mol Cell Biol. 1994; 14(10):6597–6606. DOI: 10.1128/MCB.14.10.6597 [PubMed: 7523855]
57. Vickers MF, Yao SY, Baldwin SA, Young JD, Cass CE. Nucleoside transporter proteins of Saccharomyces cerevisiae. Demonstration of a transporter (FUI1) with high uridine selectivity in plasma membranes and a transporter (FUN26) with broad nucleoside selectivity in intracellular membranes. Journal of Biological Chemistry. 2000; 275(34):25931–25938. DOI: 10.1074/jbc.M000239200 [PubMed: 10827169]
58. Rouillon A, Surdin-Kerjan Y, Thomas D. Transport of sulfonium compounds. Characterization of the s-adenosylmethionine and s-methylmethionine permeases from the yeast Saccharomyces cerevisiae. Journal of Biological Chemistry. 1999; 274(40):28096–28105. [PubMed: 10497160]
59. Hauser M, Donhardt AM, Barnes D, Naider F, Becker JM. Enkephalins are transported by a novel eukaryotic peptide uptake system. Journal of Biological Chemistry. 2000; 275(5):3037–3041. [PubMed: 10652283]
60. Karst F, Lacroute F. Ertosterol biosynthesis in Saccharomyces cerevisiae: mutants deficient in the early steps of the pathway. Mol Gen Genet. 1977; 154(3):269–277. [PubMed: 200835]
61. Kornmann B, Currie E, Collins SR, et al. An ER-mitochondria tethering complex revealed by a synthetic biology screen. Science. 2009; 325(5939):477–481. DOI: 10.1126/science.1175088 [PubMed: 19556461]
62. Ghaemmaghami S, Huh WK, Bower K, et al. Global analysis of protein expression in yeast. Nature. 2003; 425(6959):737–741. DOI: 10.1038/nature02046 [PubMed: 14562106]

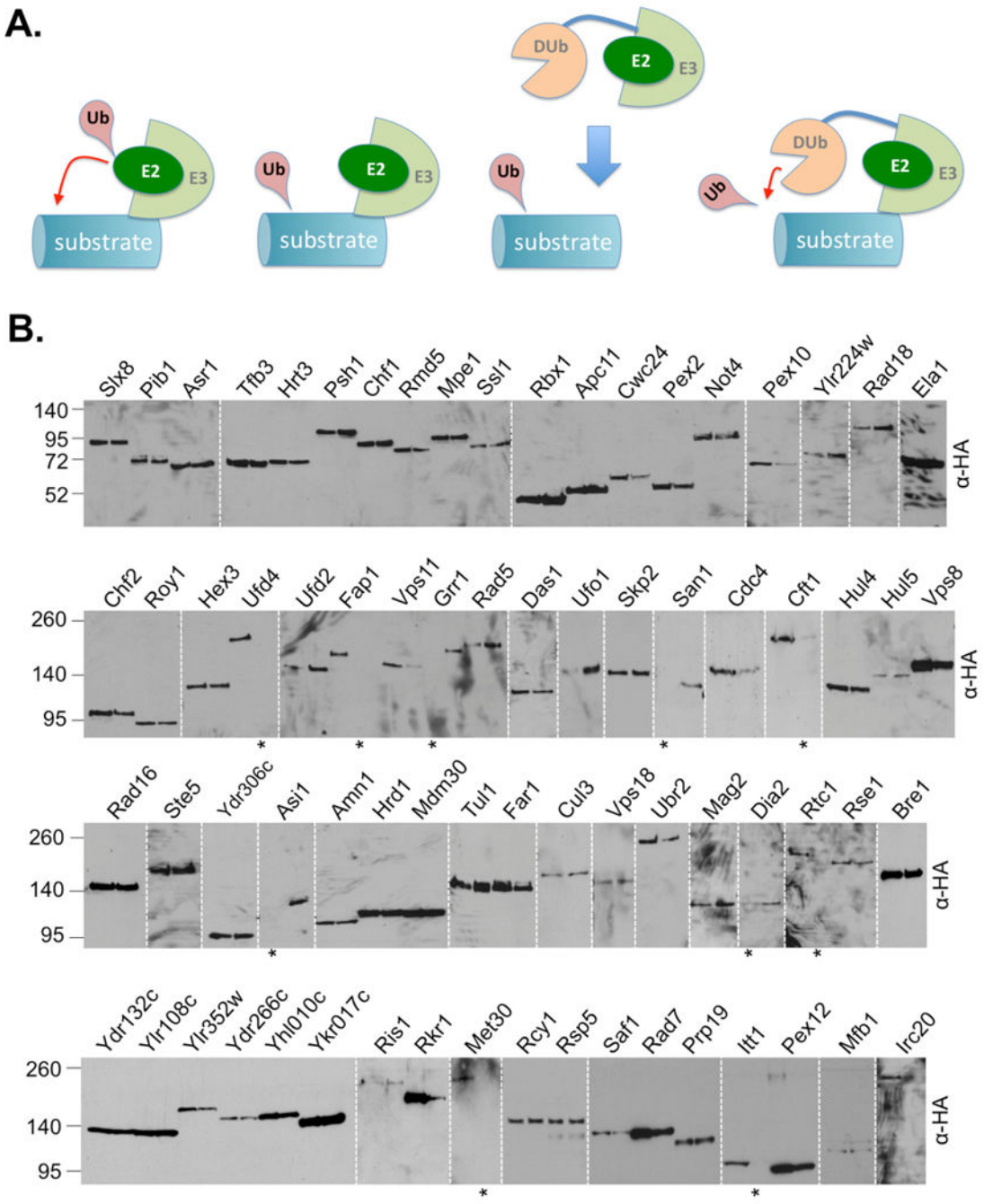


**Figure 1. A systematic plasmid library for reversal of yeast E3-ligase activity**

A) Schematic representation of ligase-DUb fusion proteins. The final step in the ubiquitination cascade involves transfer of Ub from an E2 conjugating enzyme to a substrate through the activity of an E3 ligase enzyme. Substrate deubiquitination is induced by expression of E3 ligase-DUb fusion proteins.

B) E3 ligases expressed in wild-type cells as fusions with a C-terminal DUb (UL36) enzyme and an HA epitope. 50 μM copper was added to the media to induce protein expression from the *CUP1* promoter. Two transformants for each ligase-DUb fusion were validated; a black

asterisk indicates particular fusions for which only one $Ura^+$ clone expresses. Molecular weight markers are indicated.

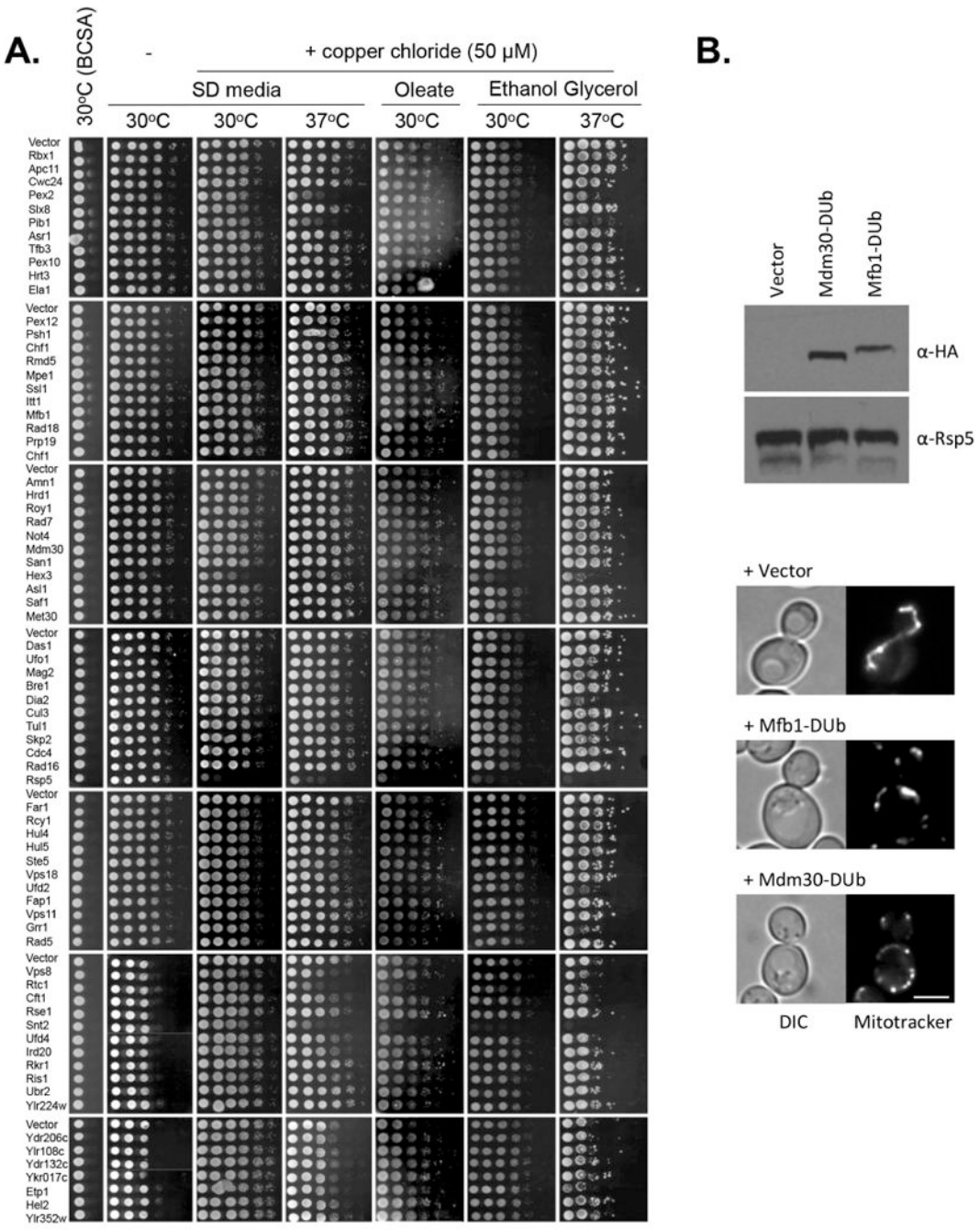


**Figure 2. Phenotypic analyses of ligase-DUb fusion library**

A) Wild-type (SEY6210) yeast cells were grown to mid-log phase in SC media lacking uracil, harvested and a 10-fold serial dilution was spotted out on plates containing different solid media. Cells were plated on media containing 50 μM bathocupriosulfonic acid (BCSA) to repress gene expression. Cells were also plated on media lacking copper or plasmid expression was induced on plates containing 50 μM copper chloride. These plates were incubated at 30°C or 37°C. Cultures were also plated on copper containing media lacking

glucose as a primary carbon source, which were instead supplied with oleate at 30°C and ethanol glycerol at 30°C and 37°C.

B) Wild-type yeast cells expressing labeled DUb fusions, or vector control, were grown to mid-log phase in standard SC-Ura media and prepared for immunoblot analysis using anti-HA and anti-Rsp5 antibodies. Cells were also grown to mid-log phase in minimal media and then labeled with MitoTracker for 1 hour, washed twice with water and then imaged by fluorescence microscopy. A Normarski image is included and 5 μm scale bars are indicated.

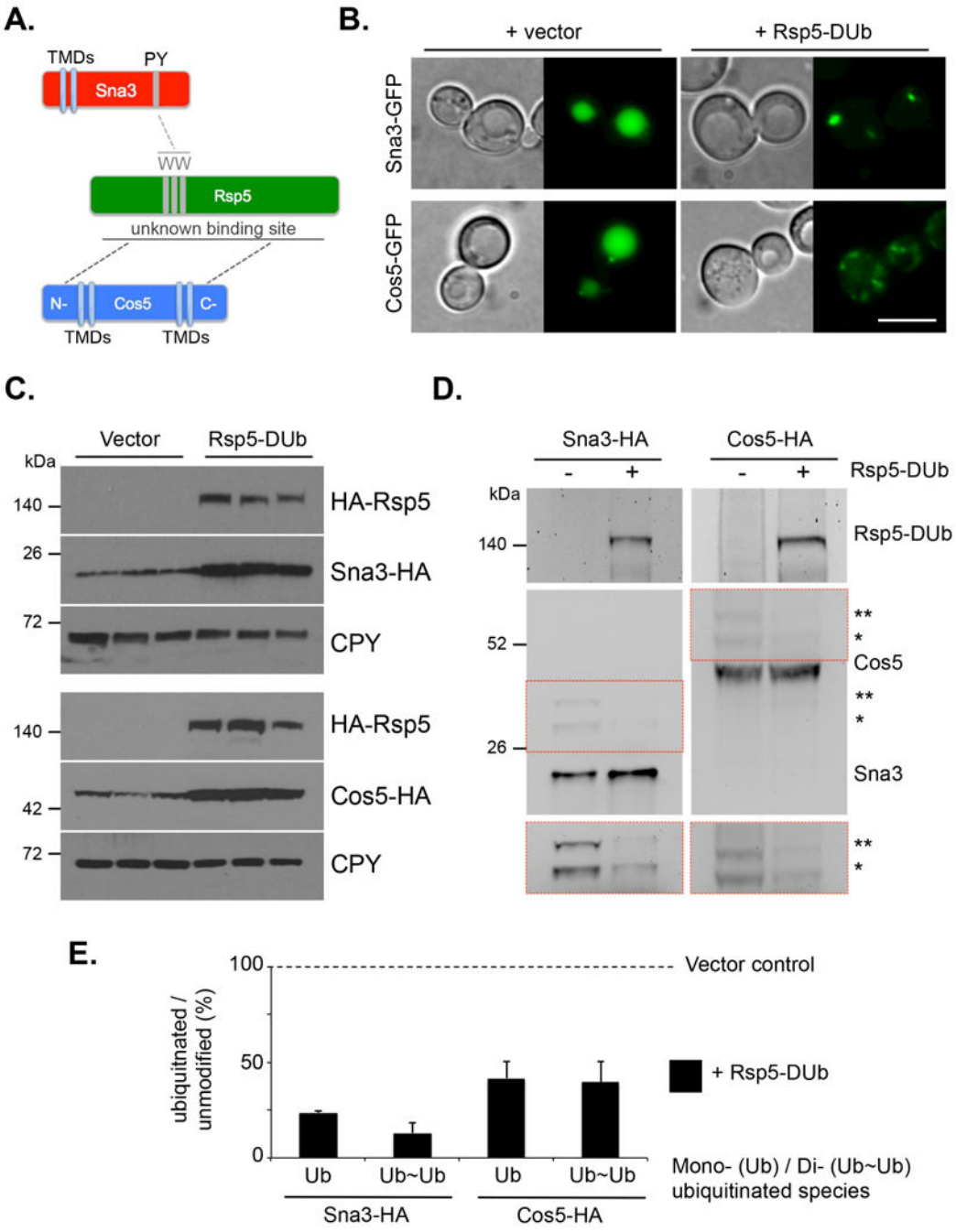


**Figure 3. Deubiquitination of Rsp5 substrates with Rsp5-DUb anti-ligase**

A) Schematic showing interactions of Rsp5 with substrates, Sna3 and Cos5. The PPxY / PY motif of Sna3 is required for interaction with the WW domains of Rsp5 (upper). The N-terminal cytosolic portion of Cos5 is sufficient to confer a ubiqutination signal for vacuolar degradation. The C-terminal cytosolic portion of Cos5 can bind directly to Rsp5.

B) Wild-type cells expressing either Sna3-GFP or Cos5-GFP were grown to mid-log phase before addition of 50 μM $CuCl_2$ to induce expression of Rsp5-DUb from the *CUP1* promoter. Cells were grown for a further 3 hours before harvesting and preparation for

fluorescence microscopy. Control cells co-transformed with an empty vector were included (left) and 5 μm scale bars are indicated.

C) Wild-type cells expressing Sna3-HA or Cos5-HA were grown to mid-log phase before induction of Rsp5-DUb for 3 hours. Cells were then harvested, lysed and prepared for immunoblot analysis with anti-HA and anti-CPY antibodies. Three transformants for each condition were analyzed.

D) HA-tagged Rsp5 substrates (Sna3 and Cos5) were expressed in *vps36Δ* cells co-expressing Rsp5-DUb (+), or co-transformed with a vector control (-), before equivalent volumes were harvested and prepared for immunoblot analysis. Unmodified Sna3-HA (left) and Cos5-HA (right) are detected in addition to the mono-ubiquitinated (*) and di-ubiquitinated (**) species of each substrate. Contrast of ubiquitnated species (red box) was adjusted to allow densitometry analysis.

E) The intensity of each unmodified, mono-ubiquitinated (Ub) and di-ubiquitinated (Ub~Ub) band for both Sna3-HA and Cos5-HA from (D) was measured using Fiji biological-image analysis software and used to ratio the level of ubiquitination / unmodified for each sample. The levels of mono- and di-Ub bands following expression of Rsp5-DUb are compared to vector control (100%; dotted line) and depicted as a histogram. Error bars indicate the standard deviation from 2 experiments.

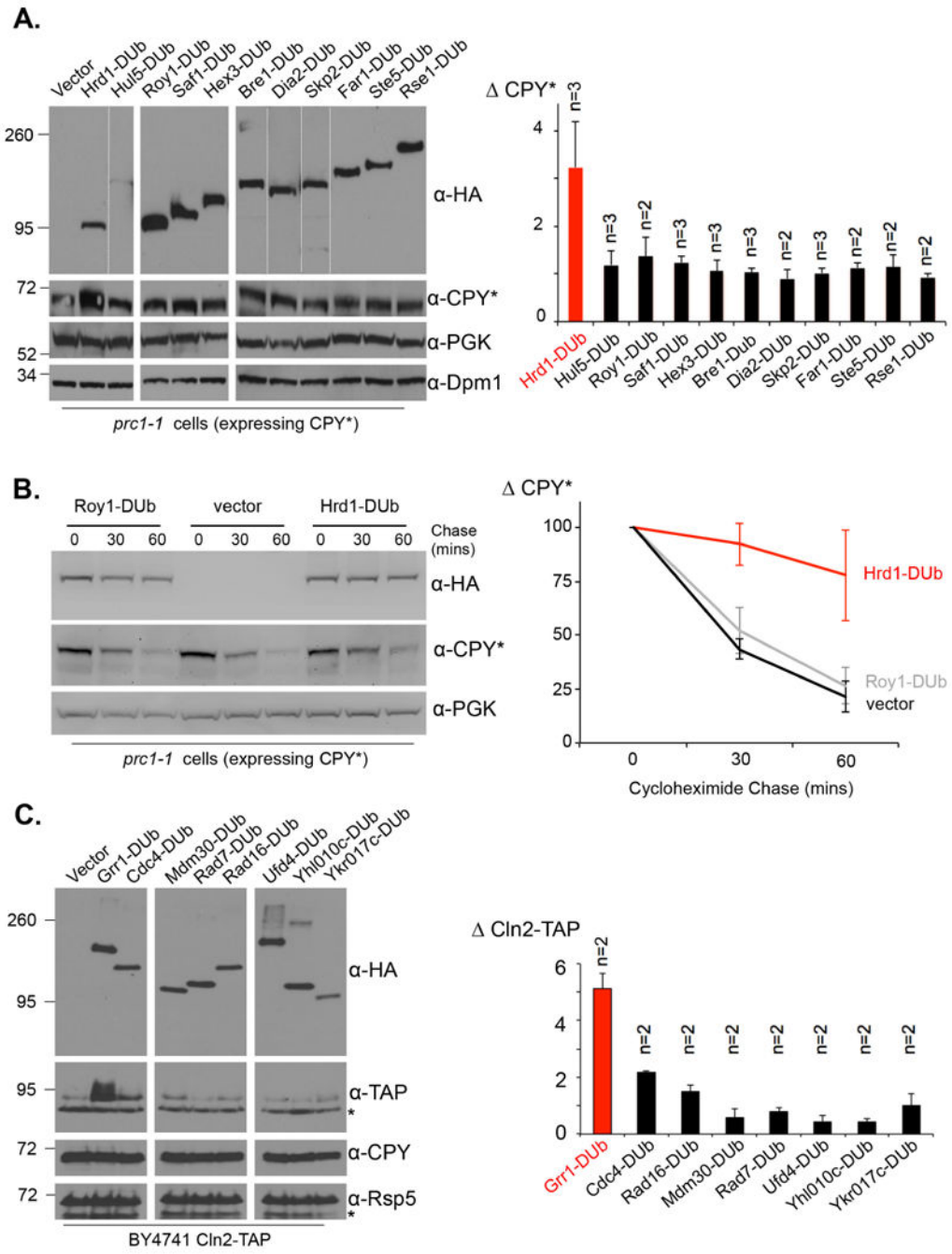


**Figure 4. Substrate specific ligase reversal**

A) Mutant *prc1-1* (CPY*) cells expressing labeled ligase-DUb fusions were grown to mid-log phase before equivalent cells were harvested from each culture. Lysates were generated by treatment with 0.2 M NaOH, resuspension in Laemmli sample buffer containing 8 M urea, followed by SDS-PAGE and immunoblot analysis using antibodies that recognize CPY*, PGK and Dpm1. Different exposures of α-HA immunoblots have been separated by spaces/dotted lines. The steady state levels of CPY* were quantified by densitometry using

Fiji software and normalized against loading control (right). Replicate number (n=) is indicated and the standard deviation shown with error bars.

B) *prc1-1* cells transformed with vector, Hrd1-DUb and Roy1-DUb were grown to mid-log phase, treated with 200 μg/ml cycloheximide before samples were harvested for immunoblotting at 0, 30 and 60 minute time-points. Resolved lysates were probed with antibodies raised against HA, CPY* and PGK. The levels of CPY* were compared to the PGK loading control using densitometry and used to plot the degradation kinetics of CPY* over time, depicted in line graph (right). The standard deviation from three experiments is shown with error bars.

C) BY4741 cells stably expressing Cln2-TAP and expressing labeled ligase-DUb fusions from a plasmid were grown to mid-log phase an prepared for immunoblot analysis with anti-HA, anti-TAP, anti-CPY and anti-Rsp5 antibodies. Non-specific bands are labeled with an asterisks (*). Cln2-TAP levels were quantified as described in (A).

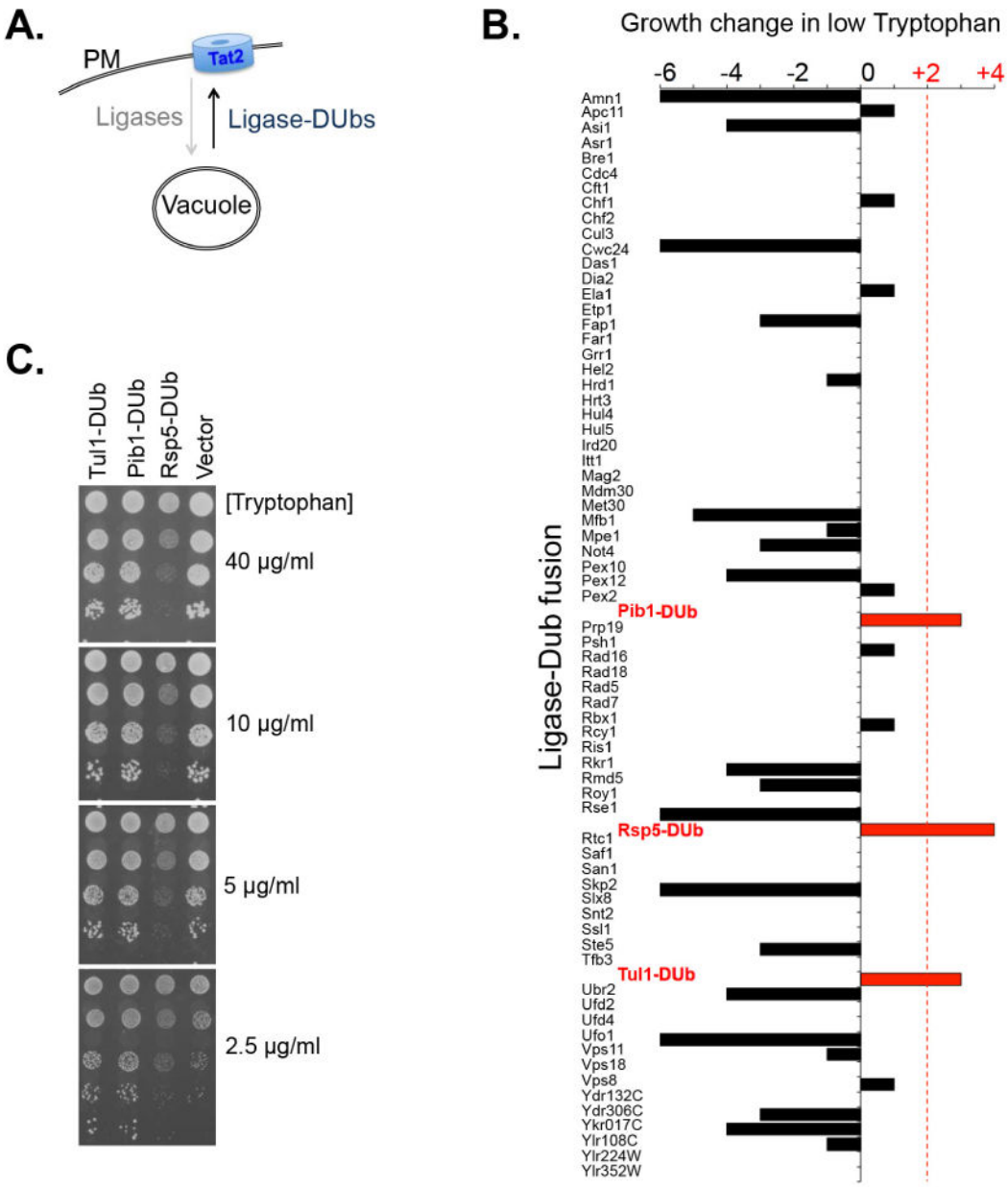


**Figure 5. Screen for ligases involved in MVB sorting using Tat2 as a reporter**

A) Schematic diagram showing how the cell surface localization of the high affinity tryptophan permease (Tat2) can be used to increase yeast cell survival when grown in restricted tryptophan conditions.

B) Growth assays were carried out in SC-Ura media containing 50 µM copper to induce expression of the DUb fusion library. An initial screen of all ligases in replete Trp (40 mg/L) and low Trp (2.5 mg/L) media was carried out. 20 ligase-DUb fusions that showed potentially increased viability in low Trp were subjected to a further series of assays on plates containing 40 mg/L, 2 mg/L, 1.5 mg/L, 1 mg/L and 0.5 mg/L Trp to establish growth enhancement more accurately. The growth advantage in low Trp was compared to growth in replete conditions and scored on an arbitrary scale between -6 (for greatest growth defect)

and +4 (greatest growth enhancement) and 0 indicating no change in growth compared with a vector control from the same plate. Ligase-DUb fusions that confer a significant growth advantage (red dotted line) are labeled.

C) Representative experiments showing the three ligase-DUb fusions (Rsp5, Pib1 and Tul1) exhibiting a concentration dependent growth advantage in limited Trp.

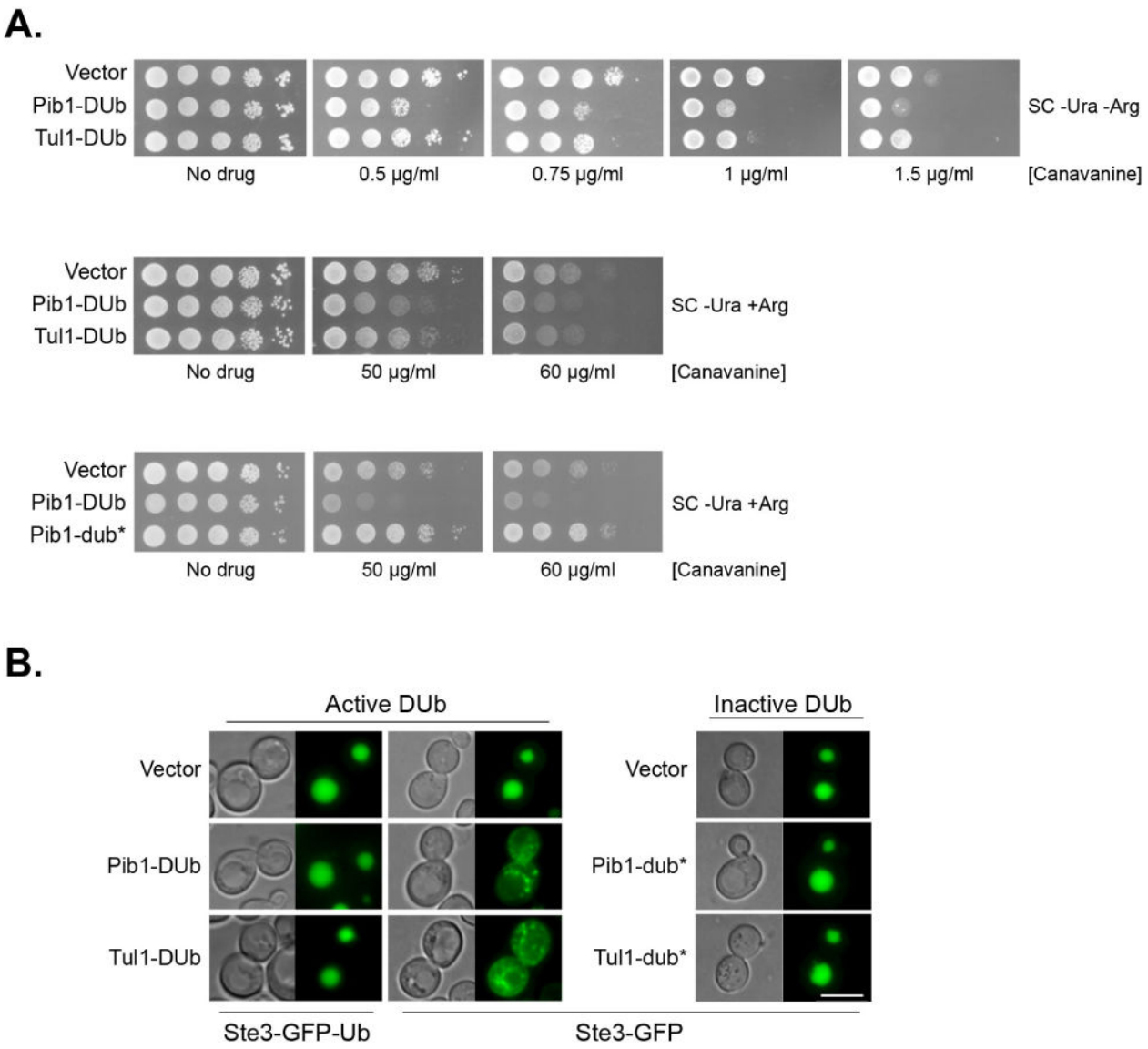


**Figure 6. Validation of ligases involved in the MVB sorting pathway**

A) Wild-type cells transformed with vector control, Pib1-DUb or Tul1-DUb were grown to mid-log phase before equivalent volumes harvested and spotted out in serial dilution (1:9) on SD-Ura-Arg media containing 50 µM copper chloride and varying concentrations of canavanine (upper). Experiments were repeated on media containing Arginine (middle), including a control set in which a catalytically dead version of Pib1-dub* was expressed (lower).

B) Cells transformed with either Ste3-GFP or Ste3-GFP-Ub alongside active and inactive versions of Pib1-DUb and Tul1-DUb were grown to mid-log phase before copper addition to induce expression of DUb-fusions. Cells were harvested and prepared for fluorescence microscopy after 2 hours. 5 µm scale bars are indicated.

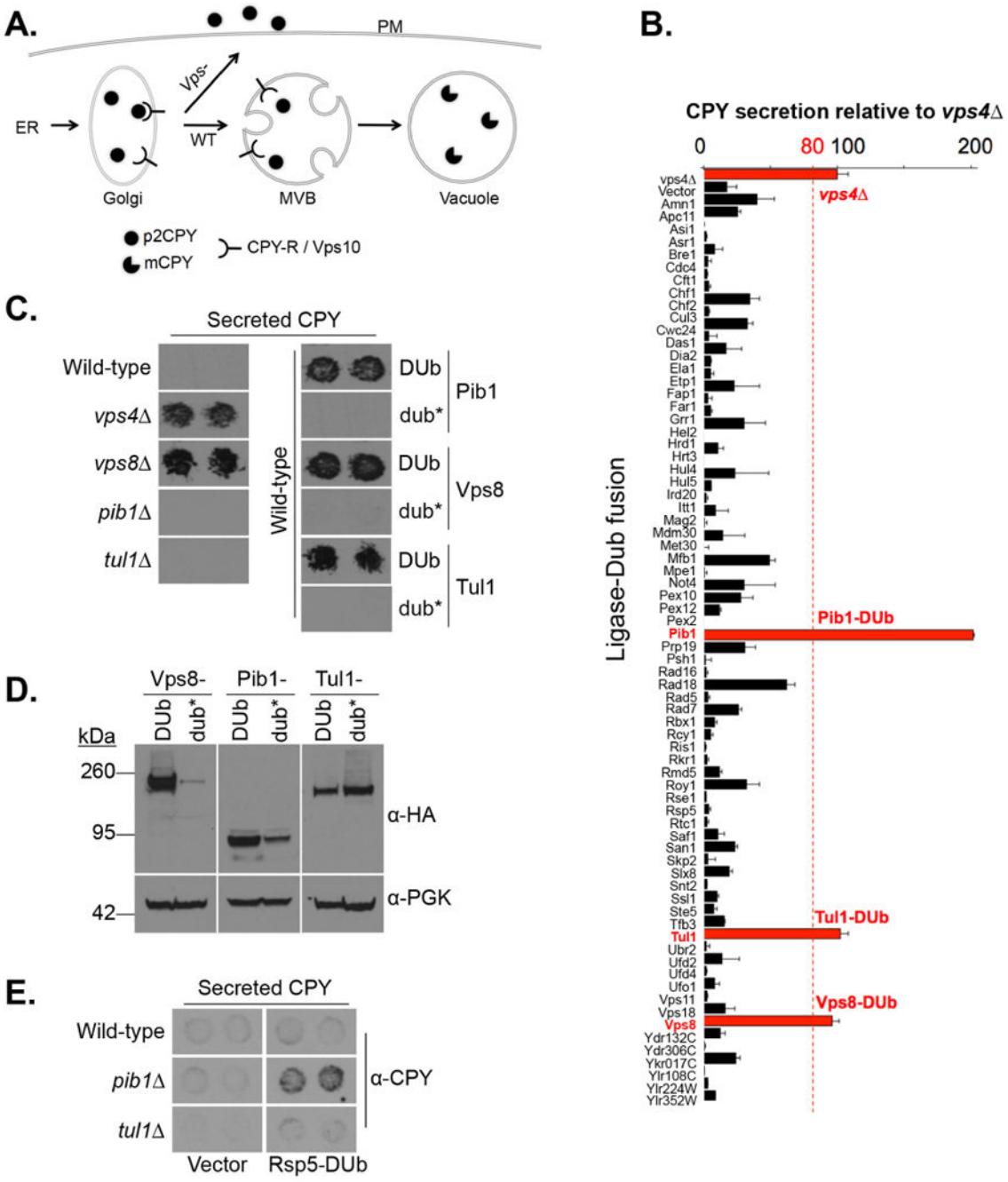


**Figure 7. Screen for ligases involved in vacuolar sorting of soluble hydrolases**

A) Schematic diagram of CPY trafficking, where newly synthesized CPY traffics to the Golgi, where it is modified to a p2-CPY precursor form (black dots) before trafficking to late endosomes, packaging into luminal vesicles at the MVB and sorting to the vacuole where it is processed to the final mature mCPY form (black circular sector). This sorting is defective in vacuolar protein sorting pathway (*vps*) mutants and p2-CPY is instead secreted from the cell.

B) SEY6210 cells expressing both clones (Figure 1B) of the DUb-fusion library were grown in the presence of copper and overlaid with a nitrocellulose membrane. Levels of secreted CPY were assessed by immunobloting the membranes with anti-CPY antibodies. All experiments contained vector controls of wild-type cells, as a negative control, and *vps4Δ* cells, which secrete >40% CPY, as a positive control.

C) Overlay experiments showing that *pib1Δ* and *tul1Δ* null cells do not secrete CPY, unlike *vps4Δ* and *vps8Δ* cells. However, expression of dominant anti-ligase versions of Pib1, Tul1 and Vps8 all secrete CPY, an effect that relies on the catalytic activity of the DUb fusion (dub* versions express a catalytically dead Cys>Ser mutant version).

D) Expression of DUb fusions, and catalytically dead (dub*) versions, was assessed by immunoblot analysis of lysates generated from cells incubated in media containing copper for 2 hours.

E) CPY secretion of wild-type, *pib1Δ* and *tul1Δ* cells transformed with an empty vector (left) or Rsp5-DUb (right) was assessed by immunoblotting the levels of CPY secreted onto an overlaid membrane during an overnight incubation.

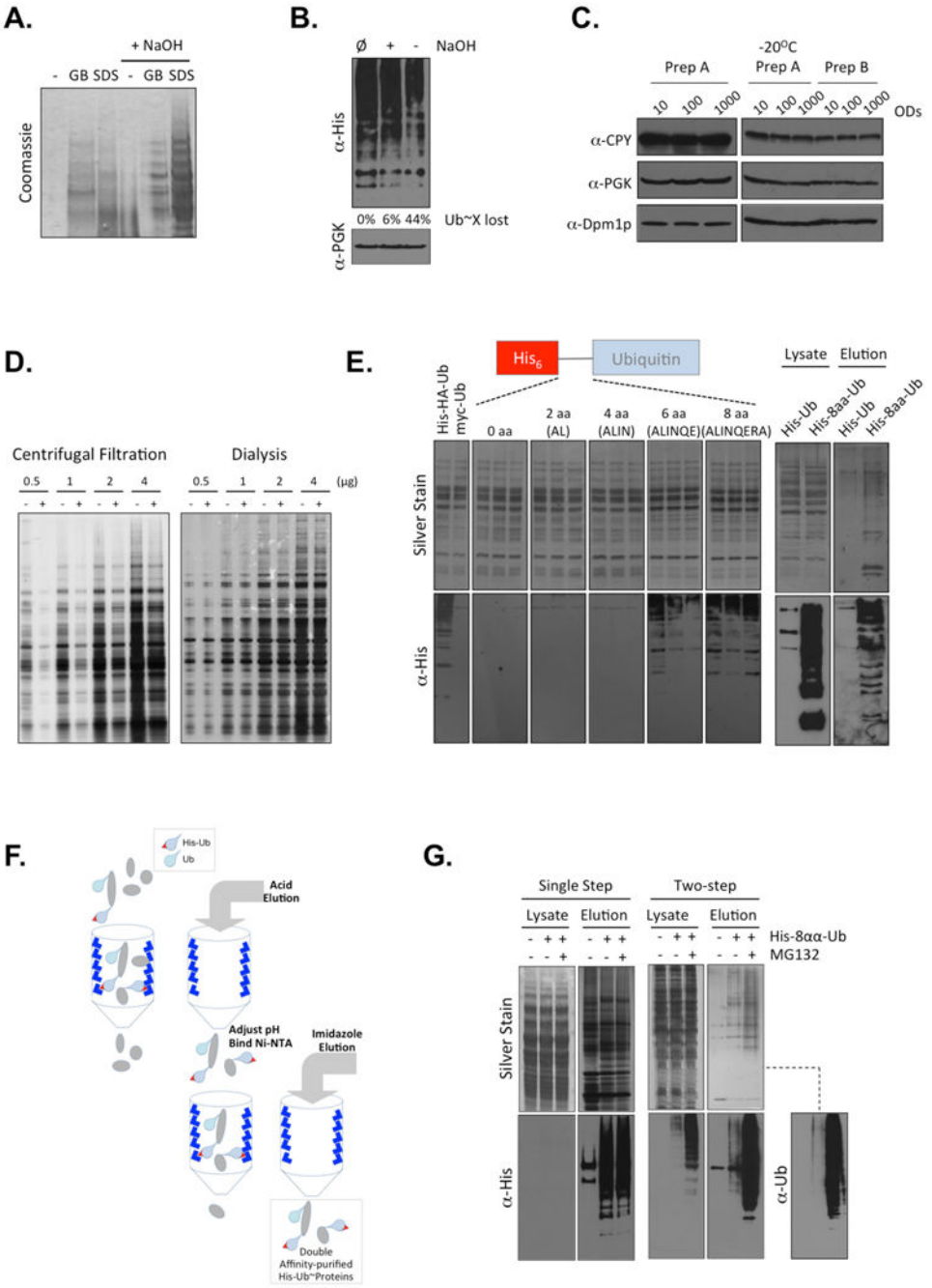


**Figure 8. Optimization of ubiquitome preparations in yeast**

A) Protein extracts were prepared by incubating harvested yeast cells in urea buffer (50 mM Tris pH 6.8, 10% glycerol, 8 M urea and bromophenol blue) either solely (-), with glass beads and vortexing (GB), or by addition of 3% SDS to buffer (SDS). Manipulations were also compared following a 3-minute incubation in 0.2 N NaOH. All lysates were analysed by SDS-PAGE and Coomassie staining.

B) Cells expressing His-HA-tagged ubiquitin were used to prepare lysates using the alkali and SDS method. Lysates were generated immediately (Ø) as in (B), or samples were treated

with NaOH for 2 minutes (+) and an untreated control (-) prior to incubation in 50 mM $NaN_3$ for 30 minutes at room temperature. Lysates were then immunoblotted using anti- His tag and anti-PGK antibodies.

C) Protein extraction methods were compared from 10 ml, 100 ml and 1000 ml cultures, using anti-PGK, anti-CPY and anti-Dpm1 antibodies. The original lysates (Prep A) were stored in -20°C freezer and then analyzed alongside fresh lysates generated from cultures of the same volume (Prep B). An equivalent number of cells amongst the lysates generated from 10 ml, 100 ml, or 1000 ml cultures were analyzed.

D) Whole cell yeast lysates were generated using lysis buffer containing 3% SDS. SDS was then removed using centrifugal filtration devices (left) or by dialyzing against lysis buffer lacking SDS (right). Different protein amounts from each sample were analyzed by silver stain before (-) and after (+) detergent removal.

E) Left, wild-type cells expressing different his-tagged ubiquitin constructs were analyzed by silver stain and immunoblot using anti-His antibodies. Different linker regions (none, 2, 4, 6 and 8 amino acids) between the $His_6$-tag and Ubiquitin were compared. Right, cells expressing His-(no linker)-Ub and His-(8 amino acid linker: ALINQERA)-Ub cells were grown to mid-log phase and lysates were generated to compare original material. These lysates were then used to perform $Ni^{2+}$-NTA affinity purifications, and the yield of protein for each transformant analyzed by silver staining and anti-His immunobloting.

F) Schematic diagram of two-step affinity purification of His-tagged ubiquitin.

G) His-Ub conjugates were affinity purified from parental control yeast cells (lacking His-Ub) and cells expressing His-ALINQERA-Ub expressed from the *CUP1* promoter. An additional sample was prepared from His-ALINQERA-Ub expressing cells that were treated with 20 mM MG-132 for 45 minutes prior to harvesting and extraction. A sample of the initial lysate was analyzed by silver stain and immunoblotting using anti-His antibodies. Purifications were performed using a 1-step protocol (see methods), that involved binding to a nickel column and elution using low pH buffer, or a 2 step protocol that involved neutralizing the initial elution, rebinding to Ni-NTA and eluting with imidazole. Immunoblot analysis of the 2-step protocol was also performed using anti-Ub antibodies.

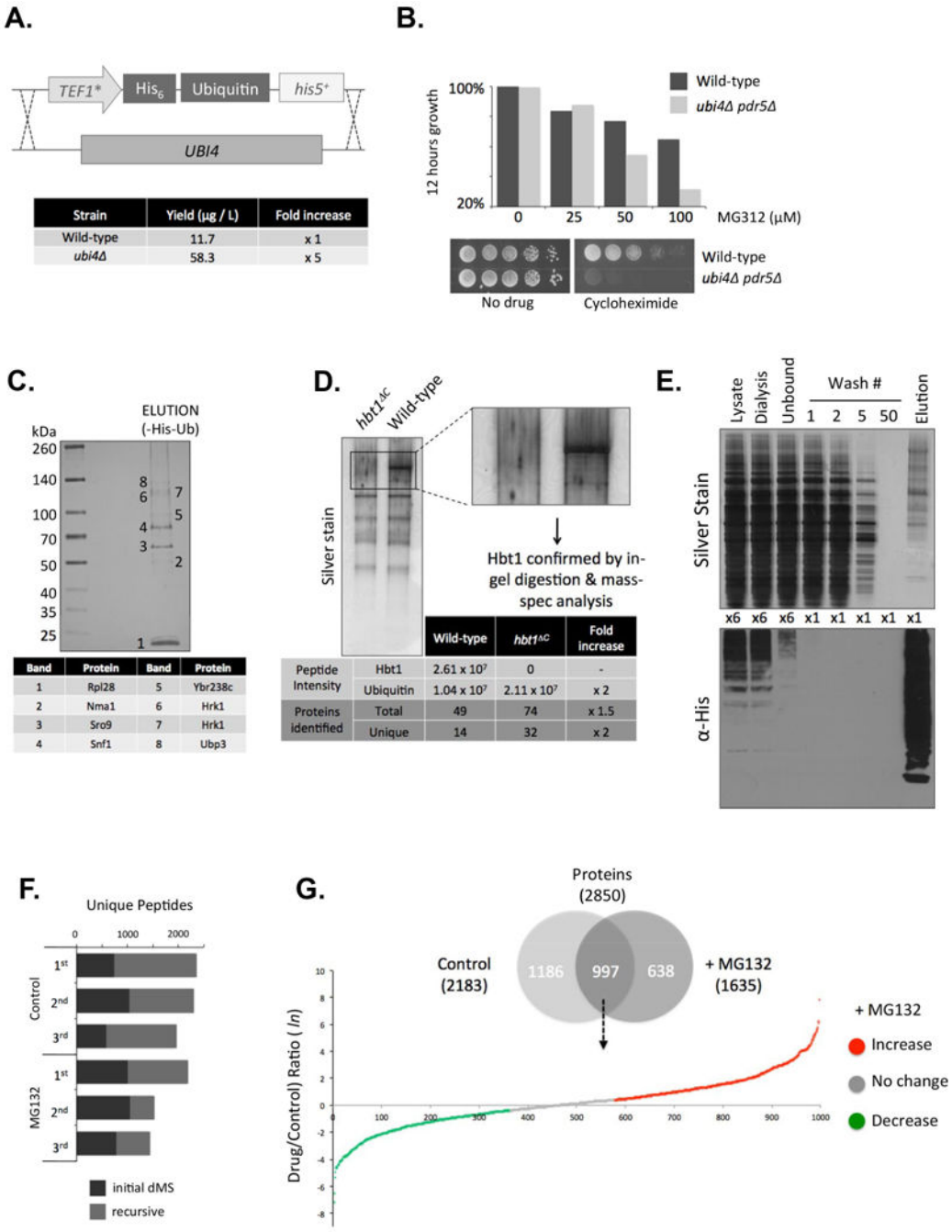


**Figure 9. Identification of ubiquitinated factors implicated in membrane trafficking**

A) Scheme for integrating the *TEF1**-6xHis-ALINQERA-Ub cassette in place of the endogenous *UBI4* gene.

B) Susceptibility of *pdr5*Δ *ubi4*Δ::*TEF1**-6xHis-ALINQERA-Ub to the proteasome inhibitor MG132 and the protein translation inhibitor cycloheximide. Cells were grown in liquid culture in the presence of the indicated concentrations of MG132. Growth was monitored by $OD_{600}$ and plotted relative to that of wild-type cells grown in the absence of

drug (upper). Cells were serially diluted and plated onto SD media or SD media containing 0.2 μg/ml cycloheximide (lower).

C) Representative His-ALINQERA-Ub purification, with samples removed at each stage and prepared for analysis by silver stain and anti-His immunoblot.

D) Affinity $Ni^{2+}$-NTA purification of lysates generated from *ubi4Δ pdr5Δ hbt1-CΔ* yeast cells not expressing His-tagged proteins. Contaminant proteins that bind strongly to the nickel column were eluted, visualized by silver stain and then identified by mass spectrometry (listed in table below).

E) Purifications of lysates generated from *ubi4Δ pdr5Δ* and *ubi4Δ pdr5Δ hbt1-CΔ* strains. The insert shows a zoomed in image of the purified Hbt1 band.

F) Yeast cells expressing His-ALINQERA-Ub were treated with MG-132, with a control untreated sample, before lysates were generated and samples were prepared for tandem MS/MS analysis. Triplicate experiments were performed for each condition. The number of unique peptides identified for the initial directed MS run (dark grey) or following recursive analyses (light grey) is depicted.

G) Proteins identified from analysis described in (F) were collated and differences following MG-132 treatment displayed as a Venn diagram (upper) and the change in protein levels following drug treatment shown (lower). Less than a 1.5 fold increase / decrease upon drug treatment was considered unaltered (grey).

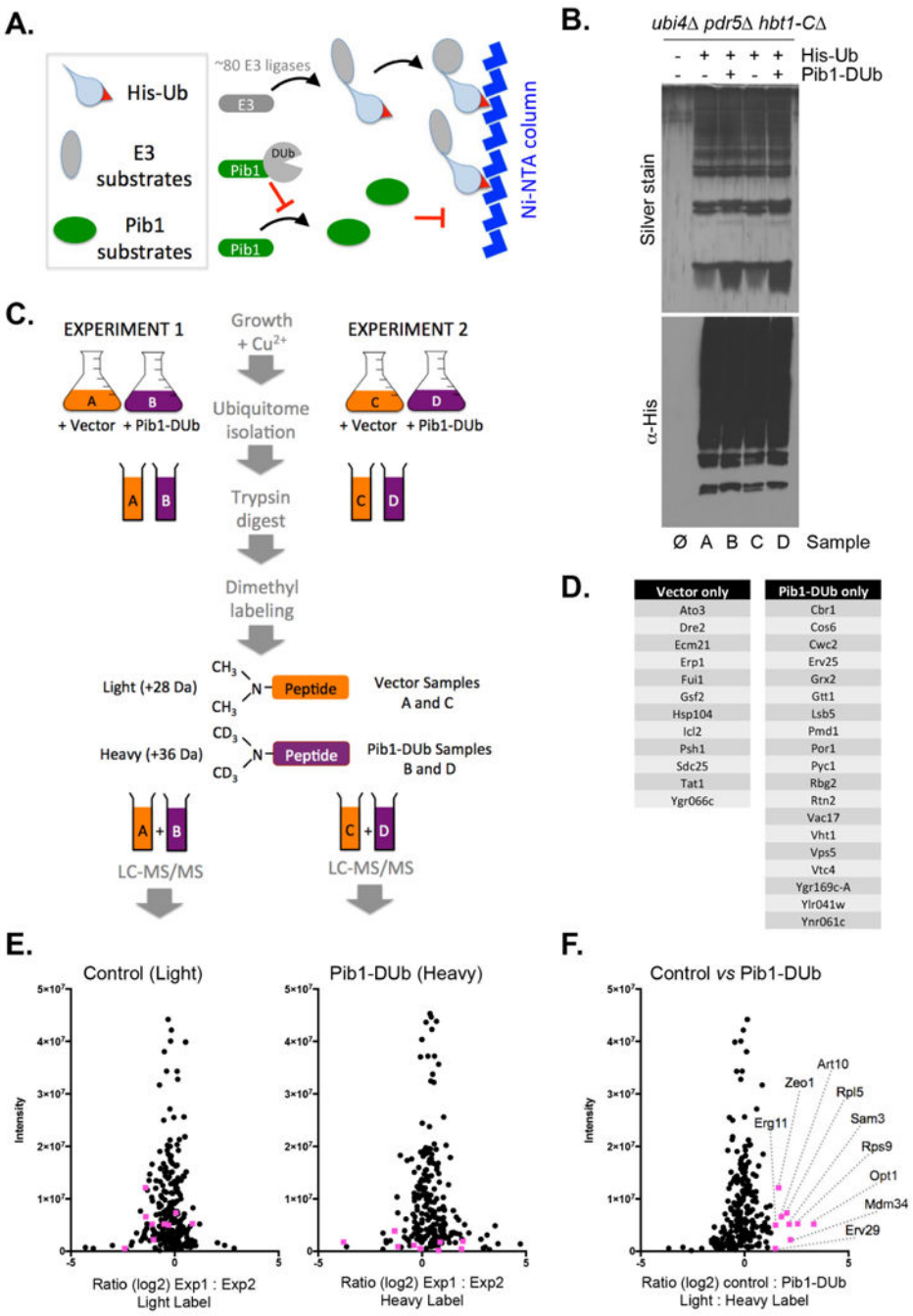


**Figure 10. Modulation of the ubiquitome following Pib1-DUb expression**

A) Schematic of ubiquitome purification from *pdr5Δ ubi4Δ hbt1-CΔ* cells transformed with vector as a control or Pib1-DUb-expressing cells, across 2 independent experiments. His-tagged Ub (His-Ub) attached to substrates (grey) facilitates binding to Ni-NTA. His-Ub conjugated to substrates of Pib1 (green) are predicted to be deubiquitinated by Pib1-DUb, thereby diminishing their recovery on Ni-NTA.

B) Ubiquitome purification from *ubi4Δ pdr5Δ hbt1-CΔ* cells not expressing His-Ub (Ø), expressing only His-Ub (vector control samples A and C) and cells co-expressing His-Ub

and Pib1-DUb (samples B and D). Samples were analyzed by SDS-PAGE followed by silver staining (upper) and immunoblotting using anti-His antibodies (lower).

C) Experimental scheme for isolation and differential labeling of the ubiquitome from control and Pib1-DUb-expressing cells. Ubiquitomes were prepared from independent experiments (1 and 2), trypsinized, and subjected to differential di-methyl labeling (28 Da light label for vector control and 36 Da heavy label for Pib1-DUb samples). Samples were then mixed at a 1:1 ratio and subjected to LC-MS/MS analysis.

D) List of proteins that were detected only in control samples (both A and C) but not detected in ubiquitome purifications following expression of Pib1-DUb (left) and proteins that were detected only in Pib1-DUb samples (both B and D), right.

E) The variability between both light labeled control experiments (left) and both heavy labeled Pib1-DUb experiments (right) is shown as a ratio of peptide intensity ($\log_2$ scale), with pink squares indicating candidate Pib1 substrates identified in (F).

F) The $\log_2$ ratio of proteins between the (light) averaged control samples and the (heavy) averaged Pib1-DUb samples. Proteins reproducibly depleted upon Pib1-DUb expression are highlighted as pink squares.

**Table 1**

**$Ni^{2+}$-NTA contaminants from yeast cell lysate**

| Band | Protein | MW (kDa) | Unique Peptides | Coverage | Abundance (Mol. / cell) | Histidine content | Possible native His tag |
|---|---|---|---|---|---|---|---|
| 1 | Rpl28 | 17 | 15 | 74% | N/A | 6.7% | Not obvious |
| 2 | Nma1 | 46 | 29 | 39% | 5127 | 5.2% | $K^{60}$-HHHHHHH-$S^{68}$ |
| 3 | Sro9 | 48 | 101 | 66% | 8424 | 3.9% | $P^{173}$-HHRNHHHSHHH-$N^{185}$ |
| 4 | Snf1 | 72 | 45 | 27% | 589 | 4.9% | $S^{17}$-HHHHHHHHHHHHHH-$G^{31}$ |
| 5 | Ybr238c | 84 | 33 | 36% | 2083 | 5.1% | $N^{98}$-HHNNNRNHHH-$N^{109}$ |
| 6 | Hrk1 | 86 | 51 | 32% | 299 | 6.2% | $F^{10}$-HGHHNDHHH-$D^{20}$ & $Q^{697}$-HHHHQH-$Q^{654}$ |
| 7 | | 102 | 30 | 26% | | | |
| 8 | Ubp3 | 114 | 25 | 24% | 2205 | 3.2% | $A^{249}$-HHHTKSH-$S^{256}$ |
| Not shown | Hbt1 | - | - | - | N/A | 4.5% | $K^{966}$-HHHNHHRH-$S^{975}$ |

MALDI-TOF identification of protein bands from Figure 9C, which were generated following affinity purification of parental strain *ubi4Δ pdr5Δ hbt1-CΔ* (not expressing His-tagged ubiquitin) on $Ni^{2+}$-NTA agarose resin. Relevant identification information, abundance and histidine content is also included, which likely explain protein affinity to resin. Details of the Hbt1 are also included, although the *hbt1-CΔ* truncation successfully removes this contaminant from purifications and the protein was not detected on silver-stained gel processed for MALDI-TOF analysis.

## Table 2

**Vps proteins identified by mass spectrometry of yeast ubiquitome**

| Protein | Distinct Peptides | Ubiquitination sites |
|---|---|---|
| Vps2 | 4 | K51, K52 |
| Vps3 | 1 | |
| Vps8 | 2 | K967 |
| Vps10 | 2 | |
| Vps11 | 2 | K395 |
| Vps13 | 4 | K835 |
| Vps16 | 3 | K25, K639 |
| Vps17 | 4 | K424 |
| Vps18 | 2 | |
| Vps20 | 2 | K42, K46 |
| Vps21 | 1 | |
| Vps22 | 1 | |
| Vps23 | 1 | |
| Vps28 | 1 | K211 |
| Vps30 | 1 | |
| Vps34 | 1 | |
| Vps39 | 2 | K263 |
| Vps45 | 2 | K17, K21, K35, K40 |
| Vps52 | 1 | |
| Vps53 | 3 | |
| Vps54 | 2 | |
| Vps65 | 1 | |
| Vps70 | 1 | K87 |
| Vps72 | 5 | K329, K162, K164 |

List of *vacuolar protein sorting (Vps)* proteins and ubiquitnation sites identified from Figure 9G.

## Table 3
### SNARE proteins identified by mass spectrometry of yeast ubiquitome

| Protein | Distinct Peptides | Ubiquitination sites |
|---|---|---|
| Sec9 | 2 | K610 |
| Sft1 | 1 | |
| Snc1 | 1 | |
| Snc2 | 1 | |
| Spo20 | 1 | |
| Sso1 | 1 | |
| Sso2 | 1 | |
| Sso1 /2 | 2 | |
| Syn8 | 1 | K28 |
| Vam3 | 1 | K113 |
| Vti1 | 2 | |
| Ykt6 | 1 | |

List of Soluble NSF Attachment Protein Receptor (SNARE) proteins and ubiquitnation sites identified from Figure 9G.